

INVESTIGATION OF A PULSED
HIGH-CURRENT DISCHARGE
WITH CROSSED
ELECTRIC AND MAGNETIC FIELDS

CARL ERIK RASMUSSEN

BIBLIOTHEEK
GORLAEUS LABORATORIA DER R.U.

Wassenaarseweg 76
Postbus 75 - LEIDEN

Universiteit Leiden



2 056 346 1

Bibliotheek
Gorlaeus Laboratoria
Universiteit Leiden
Postbus 9502
NL-2300 RA LEIDEN

INVESTIGATION OF A PULSED
HIGH-CURRENT DISCHARGE
WITH CROSSED
ELECTRIC AND MAGNETIC FIELDS

PROEFSCHRIFT

TER VERKRIJGING VAN DE GRAAD VAN DOCTOR IN DE
WISKUNDE EN NATUURWETENSCHAPPEN AAN DE
RIJKSUNIVERSITEIT TE LEIDEN, OP GEZAG VAN DE
RECTOR MAGNIFICUS DR. J. GOSLINGS, HOGLERAAR
IN DE FACULTEIT DER GENEESKUNDE, TEN OVER-
STAAN VAN EEN COMMISSIE UIT DE SENAAAT TE VER-
DEDIGEN OP WOENSDAG 14 JANUARI 1970 TE KLOKKE
15.15 UUR

DOOR

CARL ERIK RASMUSSEN

GEBOREN TE BANDUNG, INDONESIA, IN 1939

PROMOTOR : PROF. DR J. KISTEMAKER

Dit onderzoek is gedeeltelijk verricht onder
leiding van Dr F.G. Insinger.

This work was performed as a part of the research program of the association agreement of Euratom and the 'Stichting voor Fundamenteel Onderzoek der Materie' (Foundation for Fundamental Research on Matter - F.O.M.) with financial support from the 'Nederlandse Organisatie voor Zuiver-Wetenschappelijk Onderzoek' (Netherlands Organisation for pure Scientific Research - Z.W.O.) and Euratom.

VI III
S T E L L I N G E N

behorend bij het proefschrift van C.E. Rasmussen

I VI

Wasa en Hayakawa schrijven de plasmavorming in hun Homopolarontlading toe aan ionisatie door positieve ionen. Bij de ontlading in waterstof wordt echter de relatieve invloed van ionisatie door elektronen sterk onderschat.

Wasa K. en Hayakawa S. (1966) J. Phys. Soc. Japan
21, 738

Pearson G.A. en Kunkel W.B. (1962) Report U C R L -
10366, University of California.

II V

Bij de vergelijking van experimentele werkzame doorsneden voor atomaire botsingsprocessen dienen de absolute waarden en de energie-afhankelijkheid afzonderlijk te worden beschouwd. De door Kieffer en Dunn gevolgde methode is onvolledig.

Kieffer L.J. en Dunn G.H. (1966) Rev. Mod. Phys.
38, 1

Milman Y. en Tabor J. (1967) Health Physics 13, 139

III

Een roterend kwartsplaatje is niet geschikt als fasemodulator in een laser-interferometersysteem.

IV

De lankmoedige houding van de overheid ten aanzien van "conventionele" vormen van milieuverontreiniging contrasteert sterk met het prijzenswaardig voorzichtig beleid van diezelfde overheid met betrekking tot de lozing van radio-actieve stoffen.

"Normen inzake Stralingsveiligheid" (1967),
Basisnormen Euratom.

V

De bestrijding van de luchtverontreiniging zal zich in de eerste plaats dienen te concentreren op vermindering van de geloosde hoeveelheden schadelijke stof, aangezien verhoging van het emissiepunt (schoorsteen) kan leiden tot verhoging van de concentratie op een bepaalde plaats en derhalve niet als een duurzame oplossing van het probleem is te beschouwen.

Milman Y. en Tadmor J. (1967) Health Physics 13, 739.

VI

Bij het lektesten van vacuümsystemen met behulp van ionensputterpompen of ionisatiemanometers verdient het gebruik van zuurstof als testgas de voorkeur boven het vaak gebruikte helium.

VII

In systemen waarin gerichte deeltjesstromen voorkomen is het soms doelmatiger een diffusiepomp te gebruiken in plaats van een ionengetterpomp.

VIII

Het verdient aanbeveling op landelijke schaal een onderzoek in te stellen naar de genetische dosisten gevolge van de röntgendiagnostiek. De sinds kort verkrijgbare gevoelige thermoluminescentiesystemen bieden voor dit doel gunstige perspectieven.

Beekman Z.M. (1962) "Genetically significant dose from diagnostic roentgenology", Proefschrift R.U. Leiden.

Puijlaert C.B.A. (1969) Medisch Contact 24-25, 1

III
IV
Beentjes L.B. (1969) "An estimate of the genetically significant diagnostic roentgen-ray dose in the Netherlands (1967), Proefschrift R.U. Utrecht.
Attix F.H. (Ed.) (1967) "Luminescence Dosimetry", USAEC Conf. 650637.

IX

Het ware wenselijk, de Röntgen als gebruikelijke eenheid van exposie te vervangen door een goed in het MKSA-systeem passende eenheid.

"Radiation Quantities and Units" (1968)ICRU Rep. nr.11.

X

In Nederland bestaat behoefte aan een opleiding in de "Health Physics" op universitair niveau.

XI

Aan de behoefte computers te gebruiken als algemeen informatieverwerkend instrument binnen Universiteit of Hogeschool wordt onvoldoende tegemoet gekomen wanneer deze apparatuur beheerd wordt vanuit het gezichtspunt der exacte wetenschappen.

...-.-.-.-

CONTENTS

	Page
CHAPTER I - Experiments with Rotating Plasmas	1
1. Introduction	1
2. Survey of rotating plasma experiments	11
3. Rotating plasma experiments at IAS	17
FCM - laboratory, apparatus	17
CHAPTER II - Ionization and Sheath Growth in an $\bar{v} \times \bar{z}$ Discharge (Plasma Physics <u>11</u> (1969), pp. 181 - 177)	24
1. Introduction	24
2. Ionization in crossed electric and magnetic fields	26
3. Experiments	21
4. Discussion	24
A. The growth rate of the sheath	24
B. The formation time of the discharge	27
CHAPTER III - Rotating Plasmas and Gravitational Instability (Plasma Physics <u>11</u> (1969), pp. 197 - 209)	28
1. Introduction	28
2. Description of the device	28
3. General characteristics of the discharge	31
4. Rotations during the growth phase	37
5. Discussion	41
6. Summary	44
CHAPTER IV - Electron Density Measurement using a Laser Interferometer	44
1. Introduction and theory	44
2. Experiments	47

Aan Helga

Journal of the Royal Society (1959) "An analysis of the genetically
significant components of the human genome in the
Netherlands (1957)", Proceedings R.S. Acad.
Amst. Phil. Nat. (1957) "The genetic structure of
the Dutch people", p. 195-200

22

They were found to be genetically distinct from
the Dutch population as a whole and were found in
the Dutch population as a whole.

"Genetic structure of the Dutch people" (1957) p. 195-200.

23

In the Netherlands the genetic structure is
"Genetic structure of the Dutch people".

24

Genetic structure of the Dutch people is
Genetic structure of the Dutch people is
Genetic structure of the Dutch people is
Genetic structure of the Dutch people is

REFERENCES

CONTENTS

	Page
CHAPTER I - Experiments with Rotating Plasmas	7
1. Introduction	7
2. Survey of rotating plasma experiments	11
3. Rotating plasma experiments at the FOM - Laboratory, Amsterdam.	13
CHAPTER II - Ionization and Current Growth in an $\vec{E} \times \vec{B}$ Discharge (Plasma Physics <u>11</u> (1969), pp. 183 - 195)	18
1. Introduction	18
2. Ionization in crossed electric and magnetic fields	18
3. Experiments	21
4. Discussion	24
A. The growth rate of the current	24
B. The formative time of the discharge	27
CHAPTER III - Rotating Plasma and Gravitational Instability (Plasma Physics <u>11</u> (1969), pp. 197 - 209)	31
1. Introduction	31
2. Description of the device	32
3. General characteristics of the discharge	33
4. Measurements during the unstable phase	39
5. Discussion	41
6. Summary	44
CHAPTER IV - Electron Density Measurement using a Laser Interferometer	46
1. Introduction and theory	46
2. Experiments	49

	Page
SUMMARY	55
SAMENVATTING	57
CURRICULUM VITAE	59
DANKWOORD	60

CHAPTER II - Ionization and Current Growth in an \bar{X} r \bar{X} Discharge (Plasma Physics)	
18	1. Introduction
18	2. Ionization in crossed electric and magnetic fields
21	3. Experiments
24	4. Discussion
24	A. The growth rate of the current
27	B. The formative time of the discharge

CHAPTER III - Rotating Plasma and Gravitational Instability (Plasma Physics II) (1969)	
31	1. Introduction
31	2. Description of the device
33	3. General characteristics of the discharge
39	4. Measurements during the unstable phase
41	5. Discussion
42	6. Summary

CHAPTER IV - Electron Density Measurement using a Laser Interferometer	
48	1. Introduction and theory
49	2. Experiments

CHAPTER I

EXPERIMENTS WITH ROTATING PLASMAS

1. INTRODUCTION

During the last four or five decades, a considerable amount of scientific work has been devoted to the behaviour of charged particles in mutually perpendicular electric and magnetic fields. At the 2nd UN Conference on Peaceful Uses of Atomic Energy at Geneva (1958) a major part of thermonuclear research was declassified, and several research groups turned out to have adopted a crossed-field configuration for the production and confinement of a highly ionized hot plasma. Among these experiments, a well-defined class known as rotating plasmas could be distinguished (Anderson et al. 1958, Boyer et al. 1958); it is characterized by independently established electric and magnetic fields whose field lines are orthogonal in the main discharge region, which gives rise to a rotation of the plasma around the axis of the concentric electrode system. This plasma rotation can easily be understood from the equation of motion for a charged particle (charge q , mass m), immersed in an electric field \vec{E} and a magnetic induction \vec{B} :

$$m \frac{d\vec{v}}{dt} = q (\vec{E} + \vec{v} \times \vec{B}), \quad (1)$$

where \vec{v} denotes the velocity of the particle; the gravitational force and interactions with other particles are neglected. Let \vec{E} and \vec{B} be constant in space and time, and $\vec{E} \cdot \vec{B} = 0$. Now it is useful to write the velocity \vec{v} as

$$\vec{v} = \vec{v}_c + (\vec{E} \times \vec{B})/B^2 \equiv \vec{v}_c + \vec{v}_d \quad (2)$$

Substitution of (2) into (1) and expansion of the cross-

product gives

$$m \frac{d\vec{v}_c}{dt} = q\vec{v}_c \times \vec{B} \quad (3)$$

In this last expression the acceleration is always perpendicular to the velocity \vec{v}_c and \vec{B} , which describes a gyration around the magnetic lines of force at an angular frequency $\vec{\omega} = \frac{q\vec{B}}{m}$, eventually with a uniform translation along \vec{B} . Since the magnetic field does not perform work on the particle, the magnitude of \vec{v}_c depends entirely on its initial value. The velocity \vec{v} is apparently composed of a gyration \vec{v}_c (Larmor motion), and a uniform translation ('drift motion') \vec{v}_d whose direction ($\vec{E} \times \vec{B}$) and magnitude (E/B) are independent of the particle's mass and charge. For a particle which starts with velocity zero in these static, uniform fields the trajectory is a cycloid and the kinetic energies contained in Larmor and drift motion are equal (see e.g. Lehnert 1963). If the initial velocity differs from zero, the trajectory is trochoidal. In a concentric electrode geometry instead of a plane parallel configuration some corrections have to be made, but the general characteristics of the particle's behaviour remain unchanged; here the drift motion perpendicular to \vec{E} and \vec{B} causes a rotation around the axis of the electrode system, where electrons and ions rotate in the same direction and roughly at the same speed.

As already stated, the magnitudes of \vec{v}_c and \vec{v}_d are both of the order E/B which means that heavy particles acquire more kinetic energy $mv^2/2$ from the electric field. This made the principle of cross-field heating very attractive for application in thermonuclear devices, where kinetic ion energies of 10^3 to 10^5 eV are required, and

the energy of the electrons plays a secondary role, as long as it does not keep the ion energy down. Contrary to the drift motion, the Larmor motion can be regarded as a two-dimensional temperature motion, since the creation of ions by ionization occurs at random.

Elastic collisions may cause the charged particles to drop further in the potential field, where the potential energy is converted into Larmor energy since the drift energy is limited to $m(E/B)^2/2$. Furthermore, drift energy may be transferred into other degrees of freedom as a result of elastic collisions.

With these ideas in mind, a rotating plasma experiment was started after extensive theoretical studies at the F.O.M. Laboratorium voor Massaspectrografie (now: F.O.M. - Instituut voor Atoom- en Molecuulfysica), Amsterdam, in 1958.

However, the performance of those early rotating plasma machines fell short of the designer's expectations, for reasons which could not easily be foreseen at that time. In the first place, the absence of neutral particles and impurity ions in the discharge region turned out to be an essential condition for the production and containment of a hot, dense plasma. The intersection of magnetic field lines with electrodes and insulators should be subject of particular care. Furthermore, theoretical and experimental studies on plasma stability indicated that the commonly used $\vec{E} \times \vec{B}$ configurations were unstable.

Although considerable progress was made in later rotating plasma experiments the experiences at the F.O.M.-Laboratory and at other institutions made us abandon controlled thermonuclear fusion as a direct goal in our

$\vec{E} \times \vec{B}$ - machines, and concentrate our experimental studies upon the properties of the pulsed high-current $\vec{E} \times \vec{B}$ - discharge. Apart from the fusion aspects, the study of rotating plasma is very useful since the $\vec{E} \times \vec{B}$ configuration is present in many other gas discharge devices; in several 'thermonuclear' devices (e.g. theta-pinches), ion and plasma sources, and the familiar Penning vacuum gauge. More in general one can say that in most experiments where a magnetic field is used but no externally applied electric field, space charge or induction effects may give rise to a crossed-field configuration, resulting in rotation of the plasma and unstable operation of the device. This can easily happen in the sheath between a plasma and a wall. However, the phenomena observed in different $\vec{E} \times \vec{B}$ - experiments are not easily comparable, since the characteristics of such discharges depend on the electric and magnetic field strengths, gas pressure, linear dimensions and electrode geometry, filling gas and even electrode materials. The degree of ionization in a Penning cell is very low, while the gas in a high-current rotating plasma device can be fully ionized. As our experiment clearly belongs to the second type, our results will most conveniently be compared with those obtained from other rotating plasmas (see survey below). However, the concepts used on our study of the early stages of the discharge belong to the field of classical gas discharge physics, while investigations of collective phenomena leading to plasma instabilities in 'classical' $\vec{E} \times \vec{B}$ - discharges such as the Penning discharge have only been published quite recently (e.g. Knauer 1964, Schuurman 1966).

2. SURVEY OF ROTATING PLASMA EXPERIMENTS

Most rotating plasma experiments can be characterized as follows : In a concentric electrode geometry, the filling gas is brought into a highly or fully ionized state by a high-current discharge, fed by a low-inductance capacitor bank. In some cases the main discharge is preceded by some kind of preionization (e.g. an arc discharge), or plasma is injected before the application of the electric field. Usually the magnetic field is not homogeneous, but somewhat stronger near the ends of the discharge vessel ('magnetic bottle') in order to improve the containment of charged particles. In the main discharge region the magnetic field lines generally point in the axial direction, the electric field being directed radially. The energy withdrawn from the capacitor bank for the ionization of the gas, and the acceleration of the plasma causes a sharp drop of the external voltage, but after this stage little (radial) current is drawn from the capacitor bank, and the voltage across the discharge remains fairly constant. Energy is stored in the rotation of the plasma, and the device can be regarded as a 'hydromagnetic capacitor' (Anderson et al. 1959). Eventually the stored energy is increased by the parallel connection of a second capacitor bank, but the burning voltage is found to be limited to a maximum value, corresponding to

$$(E/B)_{\max} = (2V_i/m_i)^{1/2}, \quad (4)$$

where V_i is the ionization potential of the filling gas, and m_i is the ion mass (Fahleson 1961, Angerth et al. 1962). The 'limiting velocity' $(E/B)_{\max}$ is known as 'Alfven's critical velocity'; a tentative explanation of this phenomenon is given by Lin (1961).

In the early devices, the burning voltage was also limited because of secondary discharges ('internal crowbar') along insulators inside the discharge vessel. A general explanation of the internal crowbar effect has not been given (see e.g. Forsen and Trivelpiece 1964, Insinger 1965), but significant improvements have been achieved by minimizing the contact between the plasma and other material.

A convenient method for classification of various types of rotating plasma devices is to distinguish them by their length-to-diameter ratio ('long' and 'short' devices) which often characterizes the interaction between plasma and wall material.

Examples of long cylindrical machines are the Ixion (Los Alamos), Puffatron (Berkeley), Kruisvuur (Amsterdam), Ion-Magnetron (Moscow, Berkeley), the 'Hothouse'-type experiments with hydromagnetic ionizing fronts (Berkeley, Sydney, Stockholm), the Homopolars IV, V and Homopolar guns (Berkeley). Short, disk-shaped devices first known as 'Homopolars' have been operated in Berkeley, Stockholm, the Central Electricity Lab. in England and in Japan. The toroidal Homopolar III at Berkeley and 'current-loop' device at Stockholm are descendants of the early Homopolars in which the contact between plasma and walls have been greatly diminished.

Extensive surveys on rotating plasma experiments have been published by Lehnert (1962) and Tozer (1965). It appears from the work done in this field, that relatively few data are available on the mechanism of discharge build-up in rotating plasma devices, particularly where other gases than hydrogen are concerned. We are not aware of any publication in which the current growth observed in a large

$\vec{E} \times \vec{B}$ - machine is compared with available data on electron and ion impact ionization.

Another major part of our experimental work has been devoted to the study of the gravitational instability. This has not been observed in a number of $\vec{E} \times \vec{B}$ - experiments in which it was expected; a short-circuit at the endplates of the charge separation which produces the driving force of the instability has been proposed as a possible cause for the absence of the gravitational instability. In our device, where certain arrangements have been made in order to prevent internal short-circuiting, the gravitational instability is observed by means of an image converter camera. As far as we know, this method has never been employed for the measurement of instability growth rates in $\vec{E} \times \vec{B}$ - devices (the use of streak camera pictures is very common in pinch-type devices, but must in general be considered as a less powerful tool because of the optical resolution). By these unique features, our investigations take their own place among the numerous experiments in the field of $\vec{E} \times \vec{B}$ - discharges.

3. ROTATING PLASMA EXPERIMENTS AT THE FOM-LABORATORY, AMSTERDAM.

The experiments described in this thesis were carried out in an improved version of an $\vec{E} \times \vec{B}$ - device, which has been in operation until 1967. (Bannenberg et al. 1963, Insinger 1965).

In the older experiments, the cylindrical vacuum vessel (170 cm long, diameter 40 cm) was filled with hydrogen gas at a constant pressure of 5×10^{-3} mm Hg. Copper electrodes with araldite and pyrex insulation protruded axially from both ends into the vessel, the distance between the

electrode tips being one meter. Each central electrode could be connected to a separate capacitor bank (max. 18 kV, 150 μF) by means of a vacuum switch, especially developed for this purpose (Bannenbergh and Insinger 1962). The outer electrode consisted of two separate copper cylinders (length 75 cm, diameter 34 cm), firmly bolted to the stainless steel endplates of the vacuum vessel. The gap of 20 cm between these electrodes was filled up by a 40 cm long copper cylinder of larger diameter (39 cm), designed to conserve the magnetic flux when the magnetic field lines tend to bend outward as a result of plasma diamagnetism. The discharge was always operated with the central electrodes at a negative potential with respect to the grounded outer cylinders. The magnetic mirror field was provided by two sets of two copper coils, all connected in parallel, and fed from an accumulator battery with a maximum rating of 400 V, 3000 A. The magnetic induction could be kept constant during tens of milliseconds at a maximum value of 0.41 Wb/m^2 in the center of the midplane; in the center of the mirror plane the magnetic field is about twice as strong. The pumping system, consisting of an Edwards F 603 oil diffusion pump and a Speedivac 1 SC 450 B rotary pump, could maintain a background pressure of 2×10^{-6} mm Hg in the discharge vessel.

Since the formative times for build-up of the discharge were rather long at the low hydrogen pressure used, the main discharge was preceded by a preionizing arc discharge along the axis between the two central electrode rods.

Among the various experiments and technical improvements performed on this machine, the following may be mentioned : voltage and current distributions from time-

resolved measurements with movable probes and Rogowsky coils; rotational energy and density distributions from momentum transfer to small glass spheres, density measurements with a fast ionization gauge, measurements with 4 mm microwaves, and spectrographic measurements in the wavelength region 200 - 7000 Å. (Insinger 1965).

The lessons learned from these experiments led to both an extensive modification of the experimental setup, and the construction of a completely new rotating plasma device of much smaller dimensions with stronger magnetic fields. This last experiment ('Kruisvuur II') will not be discussed here.

The most important modifications on the machine were :

- a new electrode system, with central electrodes almost outside the plasma region and an outer electrode consisting of one single copper cylinder
- replacement of the vacuum switches by ignitrons
- removal of excess capacitors
- pulsed gas inlet, by means of electromagnetic gas valves built inside the central electrodes.

These modifications made the device more accessible to a great variety of diagnostics, in particular to optical, spectrographic and interferometric measurements. Furthermore, the installation had become more versatile : operation at both negative and positive polarity of the central electrodes became possible, with other filling gases than hydrogen alone.

It was decided not to use the preionizing arc (which was found to introduce a large quantity of impurities into the plasma region), in view of the efforts made to prevent any direct contact between the plasma and wall material.

As a consequence of this, most of the experiments in this device, named 'Kruisvuur (cross fire) I', could only be performed within a limited range of the applied voltage, magnetic induction and gas pressure.

REFERENCES

- Anderson O.A., Baker W.R., Bratenahl A., Furth H.P., Ise Jr J., Kunkel W.B. and Stone J.M. (1958) Proc. 2nd Int. Conf. peaceful Uses atom. Energy, Vol. 32, p. 155.
- Anderson O.A., Baker W.R., Bratenahl A., Furth H.P. and Kunkel W.B. (1959) J.Appl.Phys. 30, 188.
- Angerth B., Block L., Fahleson U.V. and Soop K. (1962) Nucl. Fusion Suppl. 1, 39.
- Bannenberg J.G. and Insinger F.G. (1962) Rev. Sci. Inst. 33, 1106.
- Bannenberg J.G., Insinger F.G., Rasmussen C.E. and Kistemaker J. (1963) Proc. 6th Int. Conf. Ioniz. Phenom. Gases, Paris, Vol. 2, p. 393.
- Boyer K., Hammel J.E., Longmire C.L., Nagle D., Ribe F.L. and Risenfeld W.B. (1958) Proc. 2nd Int. Conf. peaceful Uses atom. Energy, Vol. 31, p. 319.
- Fahleson U.V. (1961) Phys. Fluids 4, 123.
- Forsen H.K. and Trivelpiece A.W. (1964) Univ. of Calif., Electronics Res. Lab. Int. Techn. Mem. M - 89.
- Insinger F.G. (1965) Thesis Univ. of Technology, Delft.
- Knauer W. (1964), Hughes Res. Lab. Proposal no 64M - 3804/A 4759.
- Lehnert B. (1962) Progress in Nucl. Energy, Series IX, Vol. 2 (Pergamon Press).

Lehnert B. (1963) Dynamics of Charged Particles (North-Holland Publ. Co., Amsterdam).

Lin S.H. (1961) Phys. Fluids 4, 1277.

Schuurman W. (1966) Thesis University of Utrecht.

Tozer B.A. (1965) Proc. IEE 112, 218.

CHAPTER II

IONIZATION AND CURRENT GROWTH IN AN $E \times B$ DISCHARGE

C. E. RASMUSSEN, E. P. BARBIAN and J. KISTEMAKER
 F.O.M. Institute for Atomic and Molecular Physics, Kruislaan 407, Amsterdam,
 The Netherlands

(Received 26 June 1968 and in revised form 16 September 1968)

Abstract—The discharge buildup in a long Homopolar-type rotating plasma device with mirror-shaped magnetic field was investigated by time-resolved measurements of the current and potential distributions, in combination with image-converter camera pictures. As filling gases were used H_2 , N_2 , He, Ne and Ar at 10^{-3} mm Hg; the ratio of cyclotron and collision frequency for electrons was much larger than unity.

An exponential increase of the current was observed between 10^{-1} and 10^3 A, within a wide range of E/B . The rate of current growth in H_2 could be compared with known values of the electron impact ionization rate in crossed fields. For the other gases it is shown that under certain experimental conditions ionization by positive ions can be important.

1. INTRODUCTION

THE significance of rotating plasma devices in thermonuclear research has shifted gradually towards applications as a plasma gun (HALBACH and BAKER, 1964; FORSEN and TRIVELPIECE, 1966; STEINHAUS *et al.*, 1967). The utility of $E \times B$ -heating is subject to several limitations, in spite of interesting results obtained in Berkeley with Homopolar V (HALBACH *et al.*, 1962) and in Stockholm with the FII-device (LEHNERT *et al.*, 1966). Contamination of the plasma resulting from contact with the electrodes and 'internal crowbar' along the insulators necessitate the removal of the electric field, as soon as a sufficient degree of ionization has been obtained. Therefore, a rapid ionization of the gas is highly desirable.

The mechanism of cross-field ionization is reasonably well understood as long as space charge effects can be neglected, and full agreement between theory and experiment may be achieved after elimination of uncertainties concerning some of the collision processes. With regard to highly ionized rotating plasmas like our own experiment, there is still the need for a satisfactory explanation of the fast growth of ionization which is sometimes observed.

2. IONIZATION IN CROSSED ELECTRIC AND MAGNETIC FIELDS

The influence of a transverse magnetic field on the transport and ionizing properties of electrons has been treated by several authors, either by examination of the behaviour of single particles (SOMERVILLE, 1952; HAEFER, 1953; REDHEAD, 1958; SCHURMAN, 1966), or by studying the bulk properties of electron avalanches (BLEVIN and HAYDON, 1958; BERNSTEIN, 1962; PEARSON and KUNKEL, 1962; ENGELHARDT and PHELPS, 1963). In many respects, this influence is equivalent to an apparent increase of the pressure p , or a decrease of the electric field strength E . The relationship between the 'equivalent' and the actual pressure as derived by BLEVIN *et al.* (1958) follows from the general expression for the ionization frequency for electrons in a gas of uniform density n_0 :

$$v_i = 4\pi n_0 \int_0^\infty \sigma_i(v) v^3 f_0(v) dv \quad (1)$$

where $\sigma_i(v)$ is the cross-section for ionization by electrons with velocity v , and $f_0(v)$ the isotropic part of the electron velocity distribution. The quantity usually measured is not the ionization frequency but the first Townsend coefficient $\alpha = \nu_i/W$, W being the electron drift velocity in the direction of the electric field. In orthogonal electric and magnetic fields which are constant in space and time, this drift velocity is given by ALLIS (1956) as

$$W = \frac{(4\pi eE/3m) \int_0^\infty f_0 \frac{\partial}{\partial v} [\tau v^3/(1 + \omega^2\tau^2)] dv}{4\pi \int_0^\infty v^2 f_0 dv} \quad (2)$$

where e and m are the electron charge and mass, ω is the electron gyrofrequency eB/m , and $\tau(v)$ the mean free time between collisions of electrons with neutrals. If τ is assumed to be independent of v ($p\tau = \text{const.}$), equation (2) reduces to

$$W_{B/p, E/p} = (eE\tau/m)/(1 + \omega^2\tau^2) \quad \text{for } B \neq 0 \quad (3a)$$

and

$$W_{0, E/p} = eE\tau/m \quad \text{for } B = 0. \quad (3b)$$

When $B \neq 0$ the quantities will be denoted by an index ($B/p, E/p$), while ($0, E/p$) is used in cases where $B = 0$. Assuming now that the magnetic field does not alter the shape of $f_0(v)$ but only changes the mean energy, one may consider two equivalent cases ($B/p, E/p$) and ($0, E/p_0$) with equal mean electron energy and gas temperature. For equilibrium the energy gained by electrons during a mean free time must equal the average energy loss at collision. Because the average energy loss in the equivalent cases is identical, it follows for the energy gain that $eE(\tau W)_{B/p, E/p} = eE(\tau W)_{0, E/p_0}$. This gives the relationship between p_0 and p as derived by BLEVIN and HAYDON (1958):

$$p_0 = p(1 + \omega^2\tau^2)^{1/2}. \quad (4)$$

The integral in equation (1) is also the same in both cases with equal $f_0(v)$, since the cross-section $\sigma_i(v)$ is not influenced by the magnetic field. Therefore the ionization rates ν_i/n_0 are equal:

$$(\nu_i/n_0)_{B/p, E/p} = (\nu_i/n_0)_{0, E/p_0}. \quad (5)$$

Finally it follows from equation (3), (4), (5) and $p\tau = \text{const.}$ that the first Townsend coefficients $\alpha = \nu_i/W$ are equal:

$$\alpha_{B/p, E/p} = \alpha_{0, E/p_0}. \quad (6)$$

One might also consider two equivalent cases ($B/p, E/p$) and ($0, E_0/p$) with equal mean electron energy. A similar procedure now leads to

$$E_0 = E(1 + \omega^2\tau^2)^{-1/2} \quad (7)$$

$$(\nu_i)_{B/p, E/p} = (\nu_i)_{0, E_0/p} \quad (8)$$

$$(\alpha/E)_{B/p, E/p} = (\alpha/E)_{0, E_0/p}. \quad (9)$$

Expression (7) for the 'effective electric field' E_0 is well known in high-frequency breakdown theory, with ω denoting the radian frequency of the alternating field.

Considering the cases ($B/p, E/p$) and ($0, E/p_0$) one finds the same electron multiplication per unit of distance in the E direction, while in the cases ($B/p, E/p$) and ($0, E_0/p$)

there is the same multiplication per unit of time. Thus, the concepts of equivalent pressure and effective field are not completely equivalent.

The townsend coefficient α in the absence of a magnetic field is accurately approximated by

$$\alpha_{0,E/p} = C_1 p \exp(-C_2 p/E) \quad (10)$$

for many gases within a wide range of E/p (C_1 and C_2 being constants which depend only on the gas). Then $\nu_i/p = \alpha W/p$ in the limit of strong magnetic field ($\omega^2 \tau^2 \gg 1$) is given by

$$(\nu_i/p)_{B/p, E/p} = C_1 (E/B) \exp(-C_2^* B/E) \quad (11)$$

where $C_2^* = C_2 p \tau e/m$. This expression is obtained regardless of the concept used: equivalent pressure (combining equations 5, 3b, 4 and 10) or effective field (equations 8, 3b, 7 and 10). It shows that the ionization rate ν_i/n_0 in the presence of a strong transverse magnetic field should not depend on E and B separately, but only on the ratio E/B . Comparing equation (11) with the corresponding expression for $B = 0$,

$$(\nu_i/p)_{0,E/p} = C_1^* (E/p) \exp(-C_2 p/E) \quad (12)$$

where $C_1^* = C_1 p \tau e/m$, the variable parameter E/p is seen to be replaced by E/B when $\omega^2 \tau^2 \gg 1$ and $p\tau = \text{const}$.

When the assumptions underlying equation (11) are valid, a plot of $\log(\nu_i B/n_0 E)$ as a function of B/E at a fixed value of n_0 should be a straight line with a slope $-C_2^*$, from which the value of $p\tau$ can be deduced. The results obtained for H_2 by various authors are shown as the dashed lines (a) to (d) in Fig. 3 ($\log \nu_i/n_0$ vs. E/B) and Fig. 4 ($\log \nu_i B/n_0 E$ vs. B/E):

(a) is obtained by multiplying the experimental values for α of FLETCHER and HAYDON (1966) with calculated values for the drift velocity W .

(b) represents an extrapolation towards higher E/B of the experimental results of BERNSTEIN (1962). The difference between (a) and (b) is mainly due to a difference in W .

(c) is the result of numerical calculation by PEARSON and KUNKEL (1962), which is well approximated by a straight line in Fig. 4. Using the literature value of $130 \text{ V cm}^{-1} \text{ torr}^{-1}$ for C_2 in equation (11), the slope of the line yields a value of $p\tau$ which is in excellent agreement with the collision frequency for momentum transfer calculated by ENGELHARDT *et al.* (1963). If the line is extrapolated to the ordinate, the point of intersection gives a value for C_1 which also agrees well with the literature value of $5 \text{ ion pairs cm}^{-1} \text{ torr}^{-1}$.

(d) has been calculated by ENGELHARDT *et al.* (1963) and is seen to be almost identical to the result of Pearson and Kunkel.

As far as we know, crossed-field ionization studies have been limited to the gases H_2 , D_2 and N_2 . For gases where the collision frequency is known to be strongly velocity-dependent, a straightforward application of the equivalent pressure concept will generally lead to useless results. We observed this when calculating ν_i/n_0 for N_2 from the values for α measured by FLETCHER *et al.* (1966).

So far we have only considered mutually perpendicular fields, which are constant in space and time and not disturbed by electric currents and space charges. We did

not consider encounters between charged particles, since in our experimental conditions the relaxation times for momentum and energy transfer between charged particles are long compared with those for the most important electron-neutral and ion-neutral interactions. However, it was pointed out by LEHNERT (1966) that the growth of ionization in some similar rotating plasma experiments is too fast to be generated by electrons with a Maxwellian velocity distribution. As a tentative explanation, LEHNERT (1967) has shown how transverse density gradients in combination with the finite ion Larmor radius can produce strong space charge fields in the interior of the plasma, but we do not enlarge on this.

In the following sections we describe our measurements of the temporal growth of the discharge current in the 'Kruisvuur I' rotating plasma experiment in the current region between 10^{-1} and 10^2 A. The growth rate of the current will be compared with the ionization rate for the various gases used.

3. EXPERIMENTS

The 'Kruisvuur I' device (Fig. 1a, b) is a modification of a long Homopolar type machine with a mirror-shaped magnetic field.* In our former experiment (BANNENBERG *et al.*, 1963; INSINGER, 1965), which was conducted at a uniform hydrogen pressure of 7×10^{-3} torr, secondary discharges near the insulating end-plates ('internal crowbar') were regarded as a complication. By the use of pulsed gas inlet, internal crowbar could be avoided during the main part of the discharge in our present 'Kruisvuur' experiments. Fast-acting gas valves mounted inside the short central electrodes shoot two clouds of neutral gas towards the midplane with thermal velocity (about 1.6×10^3 m/sec for H_2).

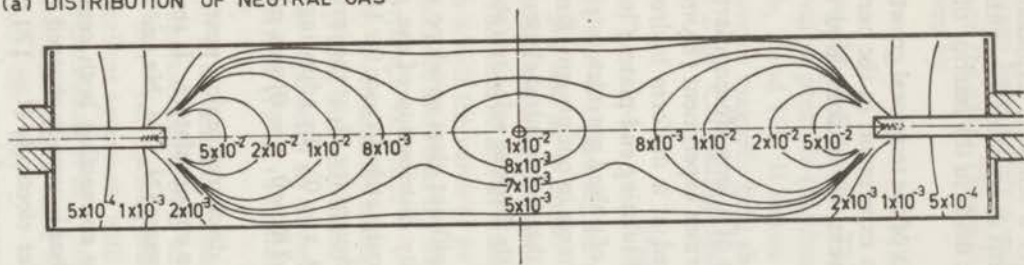
A fast ion gauge, consisting of a 6AH6 electron tube without glass envelope was used for time-resolved measurements of the spatial density distribution of the gas. The calculated time constant of the pressure gauge is approximately 40 μ sec for H_2 at 10^{-2} torr. Figure 1a shows the pressure distribution as measured for H_2 at the instant of maximum pressure in the centre of the midplane ($R = 0, z = 0$). By adjusting the energizing voltage of the gas valves, the peak pressure at ($R = 0, z = 0$) was made 1×10^{-2} torr for all gases used.

The pressure is seen to be fairly uniform in the main discharge region near the midplane, whereas the gas is efficiently kept away from the end-insulators. It seems reasonable to assume a similar distribution for the other gases (N_2, He, Ne and Ar) at the time of maximum pressure at ($R = 0, z = 0$).

This is the time when the electric field is applied by connecting both central electrodes ($l = 21$ cm, $d = 4$ cm) to a 30–60 μ F capacitor bank, usually charged to a negative voltage between 6 and 12 kV. The outer cylinder electrode ($l = 170$ cm, $d = 34$) is grounded. The vacuum potential distribution, measured in a scale model filled with electrolyte, is shown in Fig. 1b. Some field lines of the magnetic field (mirror ratio 2:1) are also drawn in this figure. During the experiment the magnetic field strength is constant in time. B_z at ($R = 0, z = 0$) can be chosen between 1200 and 5100 G; the variation of B_z with radius at a given value of z is less than 10 per cent. We used the full available range of external voltage V_0 and magnetic field strength B_z , but combinations of high V_0 and low B_z usually gave rise to unfavourable conditions for our measurements.

* For a more extensive description of the experimental setup, we refer to the companion paper by BARBIAN *et al.*

(a) DISTRIBUTION OF NEUTRAL GAS



(b) VACUUM FIELD CONFIGURATION

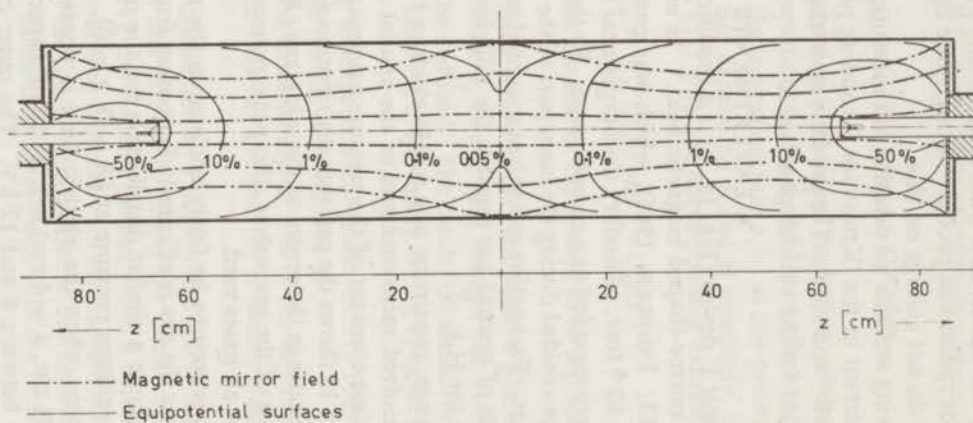


FIG. 1.—Schematic of the 'Kruisvuur I' discharge vessel with pressure and field distributions.

(a) Pressure distribution in mm Hg for H_2 -gas at time of maximum pressure at the center of the midplane ($R = 0$, $z = 0$). At this time the high voltage is applied between central electrodes (containing gas valves) and outer cylinder.

(b) Vacuum field configuration.

(---) field lines of the magnetic mirror field (—) equipotentials of the electric field (100 per cent at the central electrode).

As can be seen from Fig. 1b, the discharge starts from a vacuum field configuration with the electric vector \mathbf{E} nearly parallel to \mathbf{B} in the region around the axis. In the early stage of the discharge, electrons in this region can acquire sufficient energy to ionize the neutral gas, and a column-shaped plasma is created along the axis (phase 1).

As the plasma density increases, the direction of the electric field lines becomes radial and the magnetic surfaces become equipotentials. Potential measurements with electrostatic probes show the latter configuration to exist in the current range between 10^{-1} and 10^2 A, where our measurements were done (phase 2). Image converter camera pictures show a luminous column along the axis in this plane of the discharge. Thereafter a disk-shaped plasma is formed in the region of weak magnetic field near the midplane, mainly due to a radial expansion of the central plasma column (phase 3).

In this paper we restrict ourselves to phases 1 and 2. A detailed description of the further development of the discharge and a discussion of plasma instability during phase 2 and 3 with image converter camera pictures of all discharge phases are presented in the subsequent paper (BARBIAN *et al.*, 1969). The signal from which we derived the overall discharge voltage V_0 was obtained from a compensated resistive 1:1000 voltage divider, connected to the electrodes. The potential in the discharge region was measured with movable electrostatic probes. These consisted of a 3 mm long tungsten pin protruding from the sealed-off end of a quartz tube, and connected to a Tektronix type P6015 high-voltage probe.

The discharge current was measured with several Rogowski loops in concentric arrangement between the cylindrical electrodes: one around each central electrode, and two sets of large coils (dia. 15 and 30 cm) which could be moved in the z -direction. In this way the current was found to cross the magnetic field in a narrow region around $z = 0$. After integration the loop signals were displayed on a linear as well as on a logarithmic scale. With about 50 per cent of the shots an exponential increase of the current was measured between 10^{-1} A (the noise level) and a few times 10^2 A: $I(t) = I_0 \exp \beta(t - t_0)$. A set of typical oscilloscope traces has been redrawn in Fig. 2, where the successive discharge phases are also indicated.

The remarkable experimental fact of a constant growth factor β in a large range of current could be observed within our whole available range of the parameter E/B (from 1×10^7 to 7×10^7 cm/sec). Though some measured points scatter by a factor of two, it could be established that various combinations of E and B with the same ratio E/B did not produce a significant difference in the mean value of β .

Discharges were run in H_2 , N_2 , He, Ne and Ar with negative central electrode. Measurements with positive central electrode were done in H_2 only, because of frequent breakage of the pyrex insulator plates at this polarity. In order to study the influence of a different spatial distribution of the gas, a series of measurements was done in H_2 with the bulk of the gas still 20 cm away from the midplane.

The measured current growth rates β/n_0 (with $n_0 = 3.3 \times 10^{14}$ cm^{-3}) are given as a function of E/B by the solid curves in Figs. 3 and 4 (H_2), and Fig. 5 (N_2 , He, Ne and Ar).

For the calculation of E , the central electrode rods (radius R_1) were thought to be extended along the magnetic flux tubes. Thus the virtual central electrode has a radius $R_1\sqrt{2} \equiv R_1^*$ in the midplane, due to the mirror ratio of 2:1. We then took for E the average electric field strength between the concentric electrodes in the midplane: $E = V_0/(R_2 - R_1^*)$, where V_0 is the voltage across the discharge gap (V_0 is practically constant during the build-up phase) and R_2 is the radius of the outer electrode. If

$E(R) = V_0[R \ln(R_2/R_1^*)]^{-1}$ it follows that due to the R^{-1} dependence the strongest ionization takes place at small values of R , which contributes to the observed gradual expansion of the central plasma column.

For B we took the value in the midplane, half-way between the adopted inner and outer electrode.

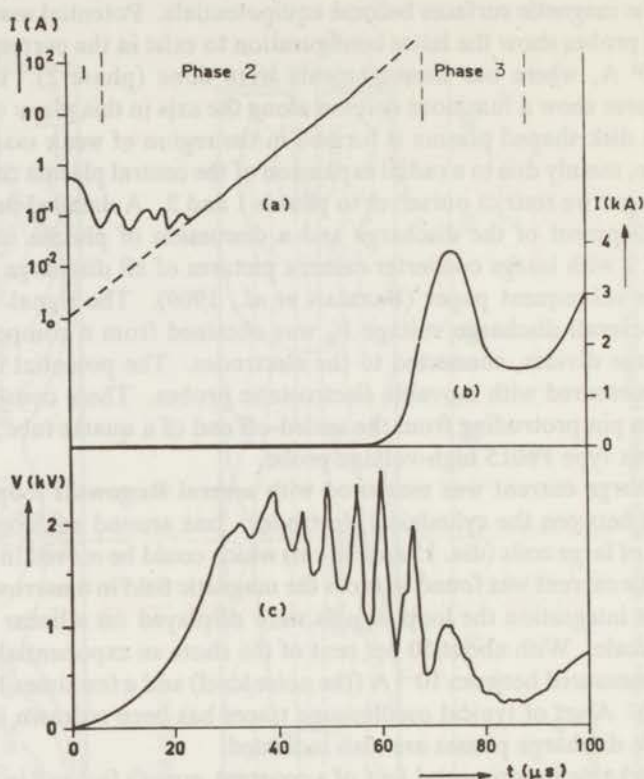


FIG. 2.—Typical signals from Rogowski coil (a, b) and electrostatic potential probe (c) for discharge in H_2 . ($E/B = 1.3 \times 10^7$ cmsec $^{-1}$, central electrode negative)
 (a) Discharge current, log. display
 (b) Discharge current, linear display
 (c) Potential probe signal at $z = 0$, $R = 12$ cm. The initial slow rise of the signal is due to the probe capacitance.

4. DISCUSSION

A. The growth rate of the current

The growth rate of the current may be identified as the mean ionization frequency, provided that:

(a) the current is representative for the growth of ionization, i.e. the electric conductivity remains proportional to the electron density and the geometry of the discharge does not change appreciably;

(b) the loss of charged particles is small compared with the rate of production;

(c) ionization of the filling gas is the dominant source of charged particles. From the observed fast exponential growth rate of the current and estimates of the outflux of charged particles we conclude that these conditions were fulfilled in most cases.

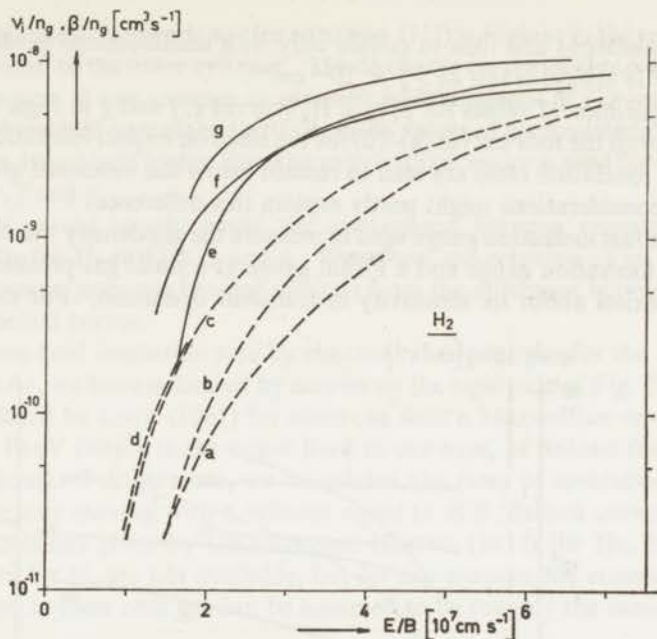


FIG. 3.—Electron impact ionization rate v_i/n_g (---) and measured current growth rate β/n_g (—) in H_2 .

v_i/n_g : (a) Fletcher-Haydon; (b) Bernstein; (c) Pearson-Kunkel; (d) Engelhardt-Phelps

β/n_g : (e) Central electrode positive, gas 20 cm in front of midplane; (f) Idem, central electrode negative; (g) Central electrode negative, gas at $z = 0$.

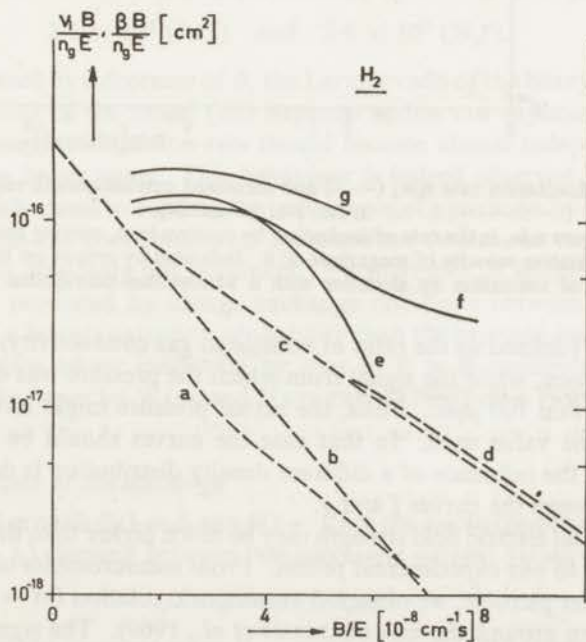


FIG. 4.— $v_i B/n_g E$ (---) and $\beta B/n_g E$ (—) vs. B/E for H_2 . The corresponding curves in Figs. 3 and 4 are labelled identically.

Assuming electrons and ions to collide only with undissociated neutral particles, the gas density is always taken as $3.3 \times 10^{14} \text{ cm}^{-3}$.

Our experimental values for β/n_0 in H_2 (curves *e*, *f* and *g* in Figs. 3 and 4) may be compared with the four curves (a)–(d) for the electron impact ionization rate ν_i/n_0 . All theoretical ionization rates are seen to remain below the measured growth rates. The following considerations might partly explain this difference:

(1) The fast ionization gauge used to measure the gas density was calibrated against a Penning ionization gauge and a Pirani gauge at a static gas pressure, but some uncertainty exists about its sensitivity in transient operation. For the tube used, the

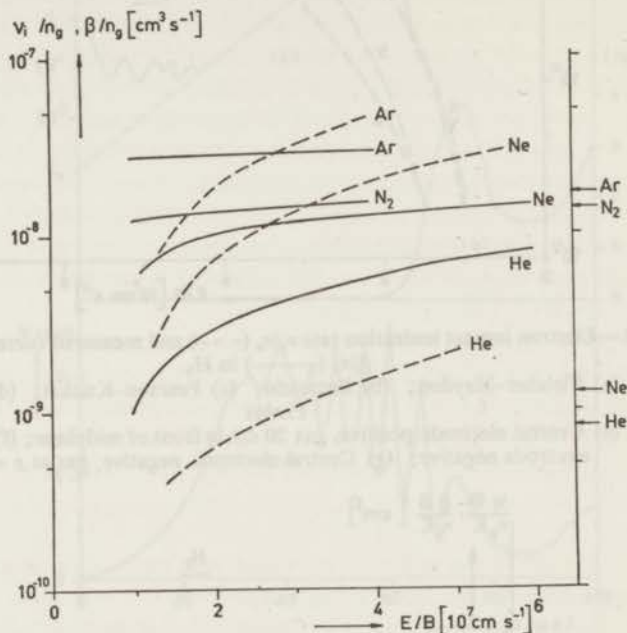


FIG. 5.—Ionization rate ν_i/n_0 (---) and measured current growth rate β/n_0 (—) in He, Ne, Ar and N_2 .

In this figure ν_i/n_0 is the rate of ionization by positive ions, moving through their own gas at a relative velocity of magnitude E/B . Indicated by arrows on the right side are the rates of ionization by electrons with a Maxwellian distribution at $T_e = 10 \text{ eV}$.

time constant (defined as the ratio of volume to gas conductivity) for H_2 at 10^{-2} torr is at least $40 \mu\text{sec}$, while the signal from which the pressure was deduced reached its peak value within $100 \mu\text{sec}$. Thus, the actual pressure might have been 10 per cent higher than the value used. In that case the curves should be shifted downward. Furthermore, the influence of a different density distribution is demonstrated by the difference between the curves *f* and *g*.

(2) The local electric field strength may be much higher than the values which have been attached to our experimental points. From measurements of E , correlated with image converter pictures, we observed an eccentric rotation ($m = 1$ instability) of the plasma column around the axis (BARBIAN *et al.*, 1969). The signal from an electrostatic probe measuring the plasma potential in the midplane shows steep fluctuations (Fig. 2c), even when the external voltage signal is smooth. The electric field strength E

and thus the ionization frequency ν_i (see equation (11)) is highest in the region where the column is closest to the outer cylinder. The discharge current will rapidly be determined by this region, if one assumes an exponential dependence of I on $\nu_i t$: $I(t) = I_0 \exp \nu_i(t - t_0)$. Averaged over many shots, the peak values of E calculated from double probe signals are 40 per cent higher than the values which we have used for our experimental curves e , f and g .

These effects would largely cover the discrepancy between experimental and theoretical results for H_2 in Figs. 3 and 4. Therefore, the presence of an anomalous ionization mechanism does not become obvious from the difference between theoretical and experimental curves.

Since the cross-field ionization rate by electrons is not known for the other gases N_2 , He, Ne and Ar, we have indicated by arrows on the right side of Fig. 5 the ionization rates calculated by LORZ (1967) for electrons with a Maxwellian velocity distribution at $T_e = 10$ eV (which is the upper limit in our case, as follows from spectroscopic observations). Furthermore, we calculated the rates of ionization by singly charged positive ions moving with a velocity equal to E/B (dashed curves in Fig. 5) from the cross-sections given by GILBODY and HASTED (1957) for He, Ne and Ar. Appropriate data for N_2 are not available, but for our purpose the cross-sections for ionization by ions in their own gas can be assumed to be roughly the same in N_2 and Ar.

In the energy range of interest, ionization by ions is a comparatively unimportant process in H_2 , but it might form a major contribution to the ionization in the other gases at higher E/B values (see Fig. 5). Of course the energy which can be present in the ion motion is limited by the applied voltage difference; the ion velocities corresponding with 10 keV are: 7×10^7 cm/sec for He^+ , 3.1×10^7 (Ne^+),

$$2.2 \times 10^7 \text{ (Ar}^+) \text{ and } 2.6 \times 10^7 \text{ (N}_2^+).$$

When E/B is increased by a decrease of B , the Larmor radii of the heavy ions approach the radial dimensions of the vessel (this happens within our experimental range of E/B) and the ion impact ionization rate should become almost independent of E/B , particularly for the heavy gases. This behaviour is indeed observed for our experimental curves, which seems to confirm the importance of ionization by ions in He, Ne, Ar and N_2 , whereas the contribution of the electrons (which we expect to depend strongly on E/B) is obviously not dominant. Furthermore, it should be noted that energetic neutrals produced by charge exchange collisions between fast ions and neutrals may have a larger ionization probability than the primary ion. As far as we know, the only place where ionization by ions in $\mathbf{E} \times \mathbf{B}$ configuration has been considered, is in the paper by WASA and HAYAKAWA (1966) on a Homopolar experiment.

B. The formative time of the discharge

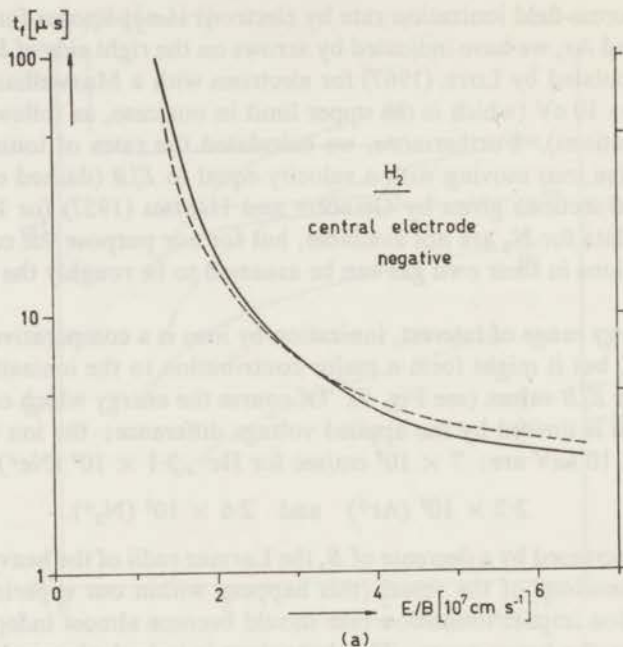
An exponential growth $I(t) = I_0 \exp \beta(t - t_0)$ of the discharge current I defines the time interval $(t_f - t_0)$ elapsing between two successive current values I_0 and I_f :

$$t_f - t_0 = \ln (I_f/I_0)/\beta. \quad (13)$$

If $t_0 = 0$ is taken as the moment when the voltage is applied it is seen from (13) that the value calculated for t_f is not very sensitive to variations of I_0 and I_f . A similar

procedure was adopted by SHERWOOD and KUNKEL (1968) when evaluating cross-field breakdown times in terms of theoretical ionization rates for H_2 .

In our case, the time necessary to reach a current I_t of 10 A could be measured directly from the oscilloscope traces used for the calculation of the current growth rate β/n_0 . Unfortunately, the rapid discharge buildup in N_2 and Ar prevented a sufficiently accurate measurement of t_t for these gases. With $I_t = 10$ A, the measured values for β and an appropriate choice for I_0 , a theoretical curve for t_t according to



(a) H_2 , central electrode negative, $I_0 = 6.3 \times 10^{-3}$ A, β as in Fig. 3f.

equation (13) was made to coincide with the experimental curve at an intermediate value for E/B (3×10^7 cm sec $^{-1}$). Within our range of E/B both curves were found to be remarkably close to each other, but for each particular gas an adequate value for I_0 had to be assumed: $I_0 = 6.3 \times 10^{-3}$ A for H_2 (Figs. 6a, b), $I_0 = 5.6 \times 10^{-4}$ A for He and $I_0 = 6.3 \times 10^{-5}$ A for Ne (Fig. 6c). A variation by one order of magnitude in these I_0 values would correspond to a variation in t_t of 30 per cent for H_2 , and about 20 per cent for Ne.

Thus, an extrapolation of the straight lines ($\log I$ vs. time) as shown in Fig. 2a intersects the vertical axis ($t = 0$) at a value I_0 of the current. It is not likely that the discharge starts with these relatively high currents. Therefore a very fast current growth must have been present in the initial phase of the discharge (phase 1). At some current value between I_0 and 10^{-1} A (the lowest current we could measure) the transition from phase 1 to phase 2 takes place; a much slower current growth sets in, and above 10^{-1} A the current growth rate is measured to be constant.

FIG. 6. (Continued)

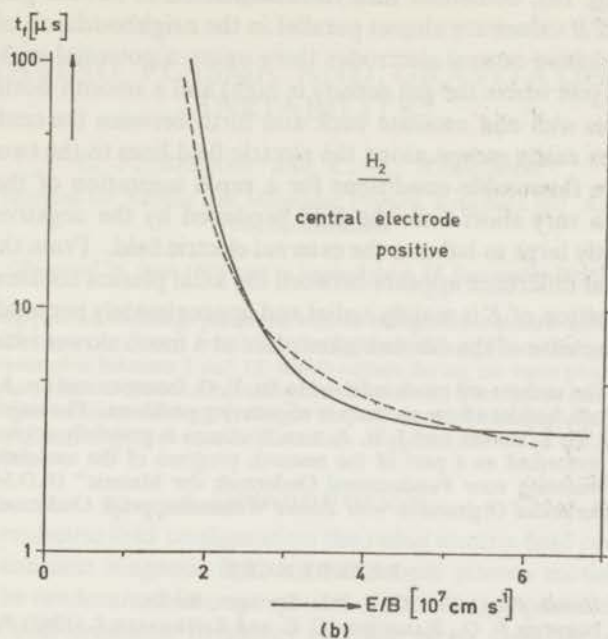
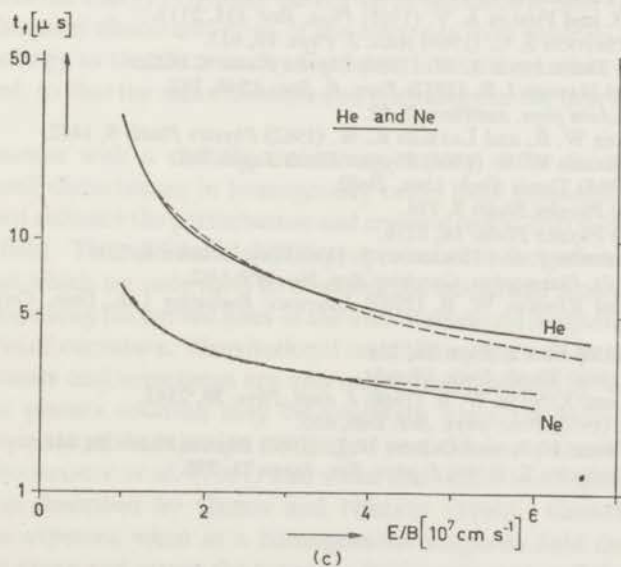
(b) H_2 , central electrode positive, $I_0 = 6.3 \times 10^{-3}$ A, β as in Fig. 3e.(c) He ($I_0 = 5.6 \times 10^{-4}$ A) and Ne ($I_0 = 6.3 \times 10^{-5}$ A), β as in Fig. 5. (central electrode negative).

FIG. 6.—Formative times t_f in H_2 , He and Ne.
 (—) time measured until current of 10 A is reached. (---) $t_f = \ln(I/I_0)/\beta$
 with $I = 10$ A and measured values for β .

The physical background of this process becomes obvious from the vacuum field configuration (Fig. 1b), combined with the distribution of neutral gas (Fig. 1a). In phase 1 the E and B values are almost parallel in the neighbourhood of the axis. Between the two negative central electrodes there exists a potential well for electrons, with steep edges (just where the gas density is high) and a smooth bottom. Electrons are trapped in this well and oscillate back and forth between the central electrodes, while positive ions easily escape along the electric field lines to the two negative electrodes. These are favourable conditions for a rapid ionization of the gas near the axis, but within a very short time the field produced by the negative space charge becomes sufficiently large to balance the external electric field. From this moment on, the entire potential difference appears between the axial plasma column and the outer cylinder; the direction of E is mainly radial and approximately perpendicular to B , so that the further increase of the current takes place at a much slower rate (phase 2).

Acknowledgments—The authors are much indebted to Dr. F. G. INSINGER and Dr. J. G. BANNENBERG for valuable discussions, besides advice and help in engineering problems. The assistance of A. BAAN, J. P. VAN DER FLUIT, H. J. TIMMER and J. H. A. VAN WAKEREN is gratefully acknowledged.

This work was performed as a part of the research program of the association agreement of Euratom and the "Stichting voor Fundamenteel Onderzoek der Materie" (F.O.M.) with financial support of the "Nederlandse Organisatie voor Zuiver Wetenschappelijk Onderzoek" (Z.W.O.) and Euratom.

REFERENCES

- ALLIS W. P. (1956) *Handb. Phys.*, Vol. 21, p. 313. Springer, Berlin.
- BANNENBERG J. G., INSINGER F. G., RASMUSSEN C. E. and KISTEMAKER J. (1963) *Proc. 6th Int. Conf. Ioniz. Phenom. Gases, Paris*, Vol. 2, p. 393.
- BARBIAN E. P. and RASMUSSEN C. E. (1969) *Plasma Phys.* **11**, 197.
- BENSTEIN M. J. (1962) *Phys. Rev.* **127**, 335, 343.
- BLEVIN H. A. and HAYDON S. C. (1958) *Aust. J. Phys.* **11**, 18.
- ENGELHARDT A. G. and PHELPS A. V. (1963) *Phys. Rev.* **131**, 2115.
- FLETCHER J. and HAYDON S. C. (1966) *Aust. J. Phys.* **19**, 615.
- FORSEN H. K. and TRIVELPIECE A. W. (1966) *Physics Fluids* **9**, 1022.
- GILBODY H. B. and HASTED J. B. (1957) *Proc. R. Soc. A* **240**, 382.
- HAEFER R. (1953) *Acta phys. austriaca* **7**, 52.
- HALBACH K., BAKER W. R. and LAYMAN R. W. (1962) *Physics Fluids* **5**, 1482.
- HALBACH K. and BAKER W. R. (1964) *Physics Fluids Suppl.* S62.
- INSINGER F. G. (1965) Thesis *Tech. Univ. Delft*.
- LEHNERT B. (1966) *Physics Fluids* **9**, 774.
- LEHNERT B. (1967) *Physics Fluids* **10**, 2216.
- LEHNERT B., BERGSTRÖM J. and HOLMBERG S. (1966) *Nucl. Fusion* **6**, 231.
- LOTZ W. (1967) *Inst. Plasmaphys. Garching Rep.* No. IPP-1/62.
- PEARSON G. A. and KUNKEL W. B. (1962) *Lawrence Radiation Lab., Univ. California, Rep.* No. UCRL-10366.
- REDHEAD P. A. (1958) *Can. J. Phys.* **36**, 255.
- SCHUURMAN W. (1966) Thesis *Univ. Utrecht*.
- SHERWOOD A. R. and KUNKEL W. B. (1968) *J. appl. Phys.* **39**, 2343.
- SOMERVILLE J. M. (1952) *Proc. phys. Soc.* **B65**, 620.
- STEINHAUS J. F., BARR W. L. and OLESON N. L. (1967) *Physics Fluids* **10**, 641.
- WASA K. and HAYAKAWA S. (1966) *J. phys. Soc. Japan* **21**, 738.

CHAPTER III

ROTATING PLASMA AND GRAVITATIONAL
INSTABILITY

E. P. BARBIAN and C. E. RASMUSSEN

F.O.M. Institute for Atomic and Molecular Physics, Kruislaan 407, Amsterdam,
The Netherlands*(Received 26 June 1968 and in revised form 16 September 1968)*

Abstract—A rotating plasma discharge produced with an independent electric field applied transverse to the magnetic field, shows an $m = 1$ instability during the buildup phase. The growth rate of a high mode instability (m -number between 5 and 15) which occurs during the main phase of the discharge is measured in dependence on the local centrifugal acceleration. The results can be compared with the theory for the gravitational modes by Chen. The influence of the Coriolis force and of finite Larmor radius effects on the growth rate is discussed. A general survey of the development of the discharge is also given.

1. INTRODUCTION

IN OUR axially symmetric field configuration the radial electric field produces together with the quasi-constant magnetic field a macroscopic plasma motion in azimuthal direction with the randomized Larmor motion of the charged particles superimposed on it. The electron cyclotron frequency is much larger than the elastic collision frequency with neutral particles which again is larger than the rotational frequency of the whole plasma column. A near Maxwellian energy distribution with a mean energy many times the energy originally picked up in the electric field can be assumed to exist due to frequent elastic collisions of the electrons with neutrals. On the other hand ions lose energy to the electrons by Coulomb interactions when a high plasma density is reached, so that the mean electron and ion energy in the first instance can be set equal.

Rotating plasmas with a radially decreasing density suffer from gravitational instabilities. Small disturbances in homogeneity cause local azimuthal electric fields which in their turn enhance the perturbation and create a radial drift motion transverse to the magnetic field. This additional drift is proportional to the gravitational acceleration $g = v^2/R$ at which we only have to consider the azimuthal plasma motion and neglect the motion along the curved lines of the inhomogeneous magnetic field because of the large radius of curvature. Gravitational instabilities are well known from quite different experiments and sometimes are also called 'flute instability' or 'interchange instability'. The plasma rotation may be moderate when the radial electric field arises as a consequence of the injection of charged particles as reported from the Ogra experiment by BOGDANOV *et al.* (1961) and when end losses become important as in the theta pinches described by GREEN and NIBLETT (1960). Generally a plasma rotation is to be expected when in a homogeneous magnetic field the transport of charged particles along and across the magnetic field produces a radial component of a potential field. In a second group of devices a radial electric field is intentionally applied as in the Ixion apparatus described by BOYER *et al.* (1958) and in the Ion Magnetron by JOFFE *et al.* (1960) or in the series of Homopolar machines in Livermore. A general survey of the work on rotating plasma devices is given by TOZER (1965).

The experiments presented here were done on an apparatus called 'Kruisvuur I' which is in many respects similar to the Homopolar V device (HALBACH *et al.*, 1962) and to the Ixion III (BAKER *et al.*, 1961) and is a modification of a previous apparatus as described by BANNENBERG *et al.* (1963) and INSINGER (1965).

In this paper we discuss the unstable phase of a rotating hydrogen plasma and investigate different parameters which can influence the growth of gravitational instabilities.

2. DESCRIPTION OF THE DEVICE

The main characteristics of the 'Kruisvuur I' apparatus (see Fig. 1) are: the quasi-static magnetic field (mirror ratio 2:1) has its maximum value of 10 kG near the top of the stainless steel central electrodes. Values between 25 and 100 per cent

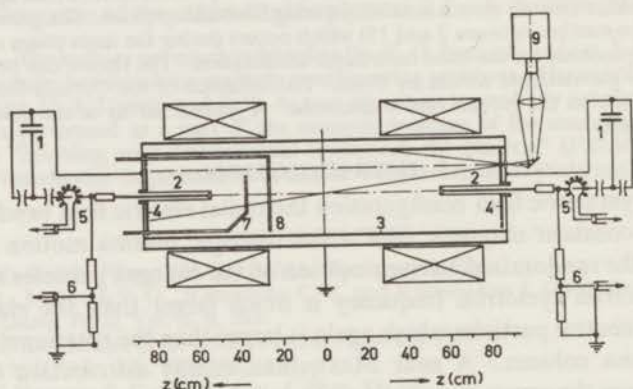


FIG. 1.—Schematic diagram of the Kruisvuur 1 device showing main circuits and diagnostic tools. Key: (1) capacitor bank; (2) central electrodes with fast gas valves which inject gas towards the midplane; (3) outer copper electrode ($R = 17$ cm); (4) Pyrex end plates; (5) Rogovsky coils for discharge current; (6) voltage divider for applied voltage signal; (7, 8) internal Rogovsky loops movable in axial direction (9) image converter camera.

of the maximum value, equal to 1250 G and 5000 G in the midplane were chosen. The magnetic field configuration is such that those magnetic field lines which graze the copper outer electrode just at the midplane, leave the vessel at the edge of the pyrex endplates at $z = 85$ cm. The outer electrode is at a radius of $R = 17$ cm which distance is equal to more than 20 ion Larmor radii at all chosen conditions. The central electrodes with a diameter of 4 cm protrude 21 cm through the isolating endplates into the vessel. This construction was chosen instead of a rigid rod as central electrode, to reduce the amount of impurities and to make the plasma at least at the center of the discharge free from viscous drag effects.

Placed inside the central electrodes are two fast gas valves which release axially directed gas pulses with a halfwidth of about $100 \mu\text{sec}$ which fill $300\text{--}400 \mu\text{sec}$ later the centre of the vessel quite homogeneously with 1×10^{-2} torr hydrogen. At the same instant the pressure in front of the insulating endplates remains still at 10^{-4} torr. This helps to retard unwanted internal short circuiting near the endplates.* When

* Drawings of the magnetic field configuration and the neutral gas distribution are given in the parallel paper concerning the ionization phase (Rasmussen *et al.*).

the neutral gas pressure has reached the desired value, two capacitor banks of $15 \mu\text{F}$ each, with the charging voltage chosen between 6 kV and 12 kV are simultaneously fired. No extra preionization is used. The energy input is chosen to provide nearly full ionization of the filling gas plus the amount needed for plasma rotation. Therefore the applied voltage decreases during the ionization phase to a fraction of the original value. This again is to reduce or avoid unwanted internal shortcircuiting when the neutral gas pressure starts to rise near the endplates later on.

The diagnostic equipment is the normal one for current and voltage measurements (Fig. 1). Double electrostatic potential probes which can be moved axially and radially make it possible to measure the local electric field strength. Inside the discharge vessel movable Rogowsky coils trace the current flow and a 3-picture image converter camera is used end-on and focussed on the midplane.

3. GENERAL CHARACTERISTICS OF THE DISCHARGE

The 'formative time' which we define for practical reasons as the time which has passed, after the discharge voltage was applied until the radial current reaches the value of 10 A, depends very strongly on the E/B ratio. With the gas pressure always at 1×10^{-2} torr, this time is as long as several tens of μsec at lower E/B values, or as short as a few μsec at high E/B values. The main characteristics of the discharge remain unchanged if E/B values are chosen between 1×10^7 and $6 \times 10^7 \text{ cm sec}^{-1}$. For this purpose the strength of the quasi constant magnetic field is chosen to be about 5000 G in the midplane and the variation of the E/B ratio is attained by different values of the electric field strength. Voltage and current signals of the discharge are given in Fig. 2(a and b). Two current maxima exist which is inherent to this kind of apparatus. The first maximum is the important one, as we will see later on. We tried to keep the second maximum small by the use of suitable values for energy input and the strength of the electric and magnetic field, such that the applied voltage has decreased to a small value after the first current maximum. A lower B -field strength results in a higher value of the radial current which again causes a faster drop of the applied voltage. This tendency is illustrated by the two different current and voltage signals of Figs. 2(a and b), where the latter shows the desired case. It should be noted that the rotational velocity at the time of the current maximum, which follows out of the E/B ratio, is roughly equal to Alfvén's critical velocity $v_A = (2V_i/m_i)^{1/2}$ when V_i denotes the ionization potential of hydrogen.

The development of the discharge can be seen to occur along several steps with gradually varying properties from one step to another. There is a

(1) preliminary phase 1: the applied electric field has still its vacuum field configuration with a strong component in axial direction. The production of charged particles is very intense compared with the

(2) buildup phase 2: the charge density has become much higher than 10^8 cm^{-3} and the electric field is radially directed because of the good conductivity in axial direction. The current growth is fairly exponential over many orders of magnitude. Movable Rogowski loops show that the radial current is directed for 90 per cent to only a 15 cm broad cylinder section of the outer electrode on both sides of the midplane. Details about the phases of ionization buildup are given by RASMUSSEN *et al.* (1969).

(3) The phase 3 between the first current maximum and the current minimum we

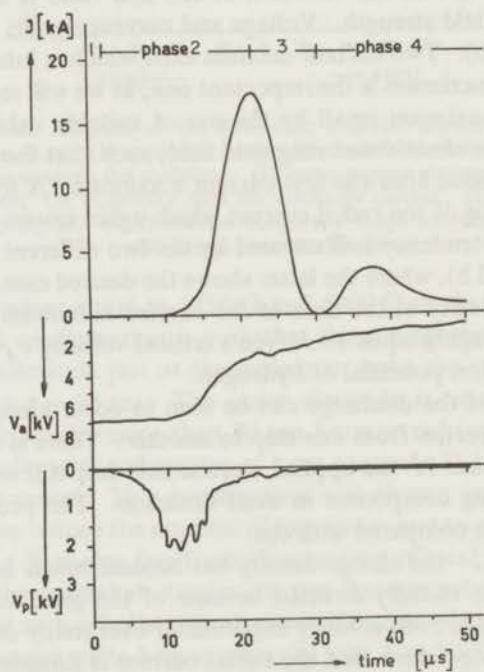
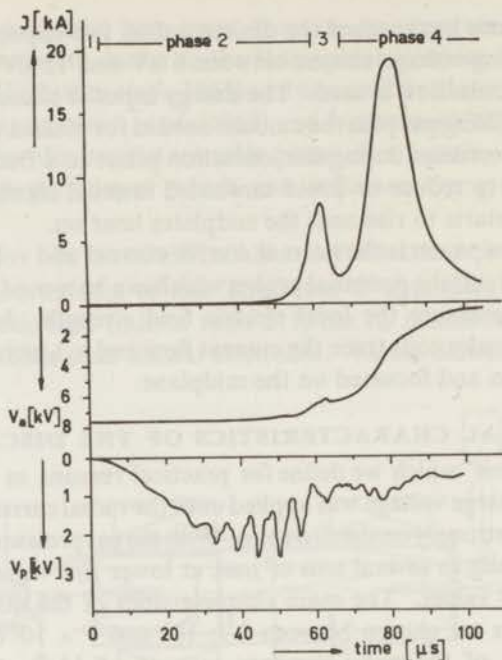


FIG. 2a, b.—Signals of the discharge current I and of the applied voltage V_a . The signal V_p shows the variation of the potential at radius $R = 13.5$ cm and at $Z = 0$. Case (a): $V_a = 7.6$ kV; $B = 5100$ G at $Z = 0$. The applied voltage decreases slowly and the signal V_p shows many oscillations. Case (b): $V_a = 6.9$ kV; $B = 4440$ G at $Z = 0$. The applied voltage decreases fastly during phase 2 and V_p shows only few oscillations. Fast buildup and large first maximum.

call the unstable phase, because of the obviously high growth rate of flute-like instabilities. In some respect also phase 2 can be considered to be slightly unstable and we will enlarge upon this later on.

(4) Phase 4, which will remain mainly out of the discussion is characterized by a second growth of the discharge current due to an additional discharge which develops near the isolating endplates and forms an internal short circuit between inner and outer electrode.

If we pursue the different phases of the discharge by means of an image converter camera, we observe during the early part of phase 2 a faint thin plasma column along the axis between the two central electrodes (Fig. 3, image 1). The fact that the ionization is stronger near the axis than elsewhere is a consequence of the configuration of the electric field as it existed during phase 1. The greatest part of the potential difference applied to the electrodes is concentrated in front of the top of the negative central electrodes, with a strong electric field component along the axis. As diffusion of charged particles transverse to the magnetic field during this short period can be neglected, the electrons oscillate back and forth in the magnetic mirror field. There are good reasons to assume that the preliminary phase lasts only for a very short time compared with phase 2 as was concluded from the investigation of the current growth by RASMUSSEN *et al.* (1969). However the distribution of charged particles as produced in phase 1 influences the distribution of phase 2. The short metal electrodes, can be considered to be prolonged along the magnetic field lines. This implies that during phase 2 after a gradual transition the applied electric field has become radially directed and is therefore transverse to the magnetic field.

This statement is affirmed by probe measurements of the radial potential distribution (Fig. 5). At the current maximum and later-on the curve of the radial potential distribution $V(r)$ shows a nearly logarithmic dependence as is expected to exist in a homogeneous medium. A similar radial potential distribution exists also during phase 2 before the current maximum, but the probe signals show strong oscillations at all radii except in the region near the axis. The maximum variations of the potential at a certain radius are within the limits V_{\max} and V_{\min} , as indicated in Fig. 5.

We now consider the time variation of a probe signal during phase 2 at $R = 13.5$ cm at the midplane and see that regular oscillations of the local potential V_p exist which disappear only after the current maximum (Fig. 2a, b). The time interval during which the oscillations can be observed is related to the time needed for the buildup of the discharge. The beginning of the signal depends mainly on the probe capacity ($C_p \approx 150$ pF). Simultaneous measurements with a low capacity pickup electrode ($C_p \approx 1$ pF) show that oscillations with smaller amplitude already start very shortly after the potential was applied. The external voltage V_a remains constant all the time.

The combination of camera observation and measurement of the radial field-strength by means of a double probe reveals that the plasma column which gradually expands during phase 2 starts an eccentric rotation with constant angular velocity which may be characterized by an $m = 1$ instability. In this connection look at the first 3 images of Fig. 3. On image (a) the plasma column is directed along the main axis. Images (b) and (c) were taken when the plasma column rotates off-axis, with a half turn between (b) and (c). When the probe remains outside the plasma column, the double probe records the maximum radial field strength at the instant

when the plasma column passes near the probe on its eccentric motion and it shows the minimum value when the plasma column is at the opposite side. The values for the radial electric field measured by double probes differ only about 10 per cent from the values which can be derived with $E = (2\pi R/\Delta t)B$ from the known radius and the measured time difference Δt between two peaks (azimuthal velocity $v_\theta = 2\pi R/\Delta t$).

As the maximum value of the radial field strength is higher than that which follows from a $1/R$ -dependence between $R_1^* = R_1\sqrt{2} = 2.8$ cm and $R_a = 17$ cm and the oscillations last for many periods, we may conclude for phase 2:

- (a) equipotential surfaces move eccentrically around the axis;
- (b) the growth rate of the $m = 1$ instability is moderate;
- (c) the locally higher than average field strength causes a higher local ionization rate which predominates over the ionization growth in other regions because of the very strong dependence of the rate of ionization on the E/B -ratio as shown by PEARSON *et al.* (1962) and RASMUSSEN *et al.* (1969).

At the beginning of phase 3 the plasma has expanded radially and after it has contracted towards the midplane a uniform plasma boundary becomes visible (Fig. 3e). On this image two thirds of the midplane where the camera is focussed upon can be surveyed. The crosswire indicates the center of the midplane. The outer ring section represents light from impurities which are released from the outer electrode surface at the small zone upon which the radial current flux falls. There is possibly also a contribution from fast neutrals produced by charge exchange processes which hit the outer wall electrode preferentially near the midplane. In Fig. 3f flute-like disturbances of a high mode type are visible which have grown out of the plasma boundary. We will discuss the growth of this instability in Section 4.

As soon as a tongue-like structure has developed the outer tip of the tongue remains back in rotation. This is due to the radially decreasing electric field and is contrary to what one might expect: the potential curve $V(r)$ (see Fig. 5) shows no abrupt change of $V(r)$ during the unstable phase, either at the visible plasma boundary, or at the outer wall. Though the measurement of the potential with an electrostatic probe is inaccurate up to several tens of volts, because the sheath potential of the probe is of the order kT/q , the percentage error remains tolerable, when the signals are in the kV range. Near the axis the potential is uniform and has the value of the applied voltage, which in our example in Fig. 5 has decreased from originally 7 kV to 6.3 kV at the time when the high-mode instability starts to grow, i.e. between the first current maximum and the current minimum. The dark hole around the axis on Fig. 3f can be explained by the small ionization rate, which exists in this region of nearly uniform potential and therefore very low electric field.

The last image (g) of Fig. 3 shows the final development during the second current maximum (phase 4). The unstable plasma has expanded already towards the outer electrode and the emission of light has considerably decreased. But very intense light comes from the region around the metal electrode, 55 cm behind the midplane. The dark hole in the center indicates the head of the electrode around which the plasma is in direct contact with the electrode surface. Again a tongue-like structure exists. Because of viscous drag the rotational velocity near the electrode surface is strongly reduced. Both, the loss of charged particles from the central mirror region and the rise of the neutral gas pressure during this later phase are probably the reason for this

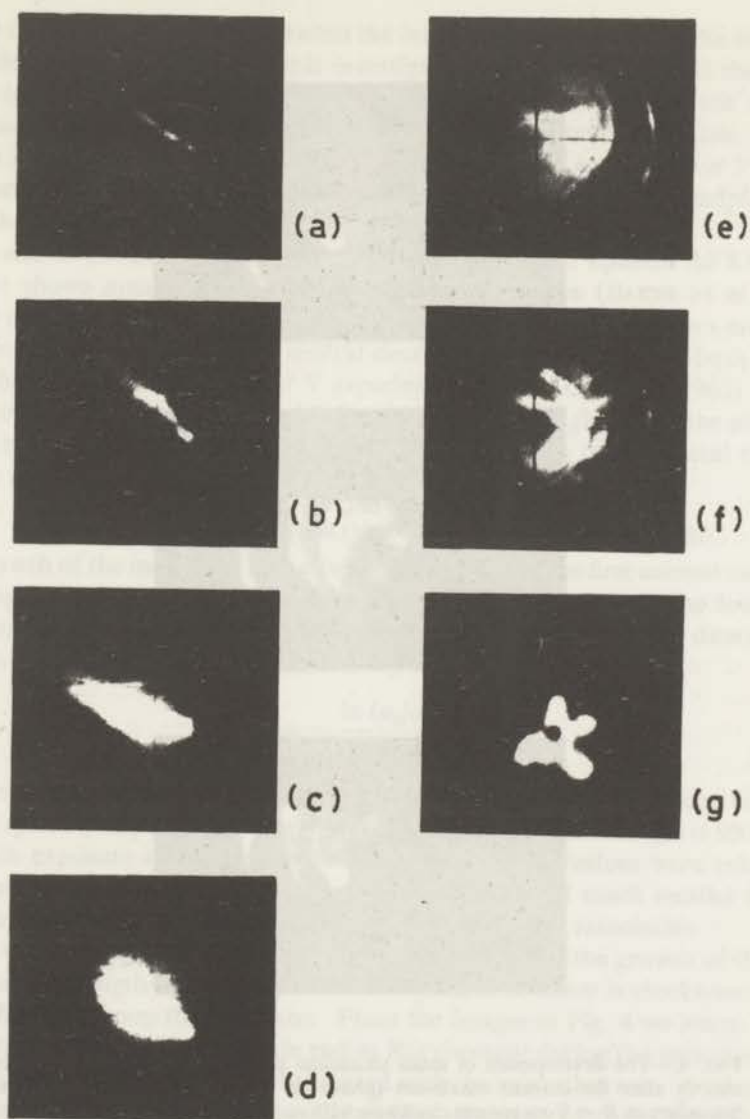


FIG. 3.--Image converter camera pictures taken during the phases 2-4. The optical axis forms a 15° angle with the central axis of the apparatus. The exposure times are about 100 nsec.

- | | |
|--|-----------|
| (a) Plasma column concentrated near the central axis. | } phase 2 |
| (b, c) Eccentric rotation of the plasma. | |
| (d) Radial expansion. | } phase 3 |
| (e) Plasma boundary is formed at $R = 10$ cm. The outer ring section represents the outer wall electrode. The cross wire indicates the center of the midplane. | |
| (f) Flute instabilities have reached great amplitudes. | } phase 4 |
| (g) Secondary discharge around central electrodes 55 cm behind the midplane. | |

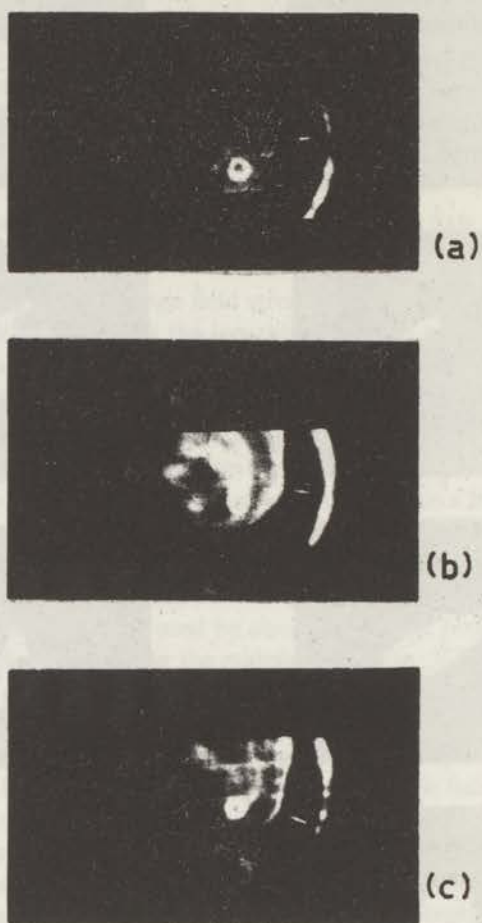


FIG. 4.—The development of small sinusoidal perturbations at the plasma boundary shortly after the current maximum (phase 3). The pictures show how the plasma boundary at $R = 9$ cm rotates clockwise with $v_{\theta} = 6.5 \times 10^6$ cm sec⁻¹. Time between exposures: $t_{1,2} = 500$ nsec; $t_{2,3} = 350$ nsec; exposure time: 50 nsec. The camera is focussed onto the midplane, the center of which is indicated by the crosswire. Small bright circle comes from the head of the central metal electrode 55 cm behind the midplane. The small arrows point towards the outmost part of the same perturbation.

secondary discharge in the space between the inner metal electrode and the surrounding wall electrode. The spectroscopic investigation of the emitted light shows that hydrogen Balmer lines are recorded during the first and second current maxima. These lines have in this experiment an observed decay time of several 100 μsec , whereas lines from impurities (mainly C, O, N) appear only at the end of phase 3 and are intense during the second maximum (phase 4). In front of the pyrex endplates and not near the midplane strong Si-lines are observed.

At the end of this descriptive part we conclude that in our opinion the Kruisvuur experiment shows many similarities to the Ixion III device (BAKER *et al.*, 1961). Especially the neutral gas injection and the formation of a central plasma column at uniform potential which acts as the central electrode are peculiarities of both devices. On the other hand, the Homopolar V experiments (HALBACH *et al.*, 1962) where a rigid rod acts as a central electrode with the gas injected through slots in the midplane, may be compared with the formation of plasma around the central metal electrode during the second current maximum of the Kruisvuur I discharge.

4. MEASUREMENTS DURING THE UNSTABLE PHASE

The growth of the instability as it develops shortly after the first current maximum was investigated by means of a 3-picture image converter camera. The local rotational velocity and the wavelength of the perturbation can be measured directly from the images. The growth rate of the instability we define by

$$\omega = \frac{\ln(a_2/a_1)}{t_2 - t_1} \quad (1)$$

where a_2 and a_1 are amplitudes of the sinusoidal perturbation of the plasma boundary at the time t_2 and t_1 respectively. The time difference between the images is 500 nsec or shorter with exposure times of 50 nsec or less. Measured values were taken only from images where the amplitude of the perturbation is still much smaller than the wavelength, so that a comparison with a linear theory seems reasonable.

Figure 4 shows in a series of three images an example of the growth of the instability. The wavelength is about 10 cm. The plasma rotation is clockwise and the camera is focussed upon the midplane. From the images in Fig. 4 we learn:

The rotational velocity at a certain radius R is constant during the period of observation. The radial motion is small compared with the azimuthal one. A remarkably distinct outer plasma boundary is visible. The diameter of the plasma is about 22 cm. Disturbances at the ill defined inner boundary seem not to be related to the perturbations at the outer side.

First, we start to compare the measured growth rates with the common flute theory as presented by LEHNERT (1961) and ROBERTS and TAYLOR (1962). If the radial wavenumber can be neglected in respect to the azimuthal wavenumber, the growth rate ω is proportional to the square root of the gravitational acceleration $g = v_e^2/R$ and the density gradient $n' = dn/dR$ divided by the density n :

$$\omega = \sqrt{\left(\frac{v_e^2}{R} \cdot \frac{n'}{n}\right)} \quad (2)$$

where the inverse of the ratio n'/n also can be interpreted as the characteristic length. Therefore ω is not very sensitive to the absolute value of the density.

We note that in this experiment only the azimuthal velocity v_θ is important for the gravitational acceleration. Even if we concede that the velocity v_\parallel along the curved magnetic field lines equals v_θ , then still the radius of this curvature is an order of magnitude larger than the plasma radius R .

The rotational velocity v_θ is a parameter which in general can easily be varied in the rotating plasma experiment by the choice of the applied voltage V_0 and the magnetic field strength B . But as to get optimal conditions the investigation of the growth rate at the plasma boundary was mainly done with values of the magnetic

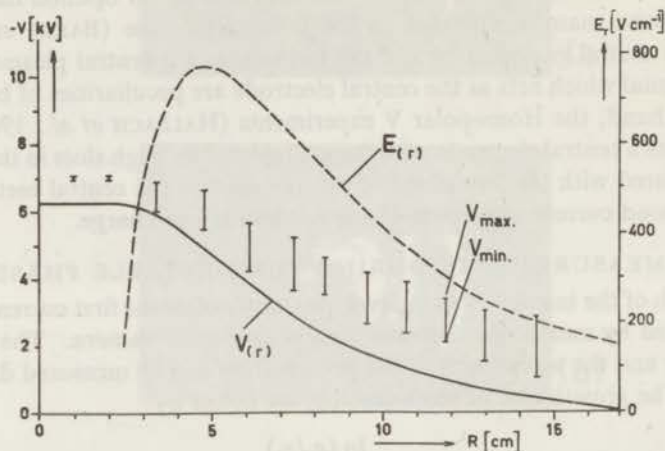


FIG. 5.—Radial potential distribution $V(r)$ and radial electric field $E(r)$ at $Z=0$ during the unstable phase 3. The vertical bars indicate the variation of the local potential $V(r)$ during the buildup phase 2. The limits V_{\max} and V_{\min} indicate the maximum and minimum values of the oscillating potential at the radius R .

field strength in the midplane between 4 and 5 kG and an applied voltage which starts from about 8 kV and decreases to 7.5 kV during the unstable phase. From the derivative of the radial potential distribution in Fig. 5 we know that the radial electric field strength decreases at $R > 7$ cm nearly proportional to $1/R$. We now tentatively relate to the visible plasma boundary the steepest density gradient of a plasma density distribution of the form $n = n_0 \exp(-R^2/R_0^2)$ when R_0 is about the outer electrode radius. This density distribution is used in the theory by CHEN (1965) which we will use for discussion later on. Furthermore, we suppose that the steepest density gradient cannot be reproduced at different shots always exactly at the same radius but builds up at arbitrary radii between $R = 8$ cm and $R = 15$ cm. Then the plasma boundary is subject to a variety of values of the gravitational acceleration $g = v_\theta^2/R$ which strongly depends on R as v_θ is proportional to the local electric field strength. In this way, we arrive at values of the gravitational acceleration between the limits $g = 14 \times 10^{12}$ cm sec $^{-2}$ at $R = 8$ cm and 1.4×10^{12} cm sec $^{-2}$ at $R = 15$ cm.

In Fig. 6 the measured values of the growth rate ω of the perturbation are plotted vs. \sqrt{g} . The diagram shows a linear increase of ω with \sqrt{g} . This result is in agreement with relation (2). To investigate the influence of the density gradient in the diagram of Fig. 7 the factor $\sqrt{(n'/n)}$ being equal to ω divided by the observed value \sqrt{g} for individual measuring points, is plotted vs. the radius of the plasma boundary R . Figure 7 shows that the characteristic length L_c which is the reverse of

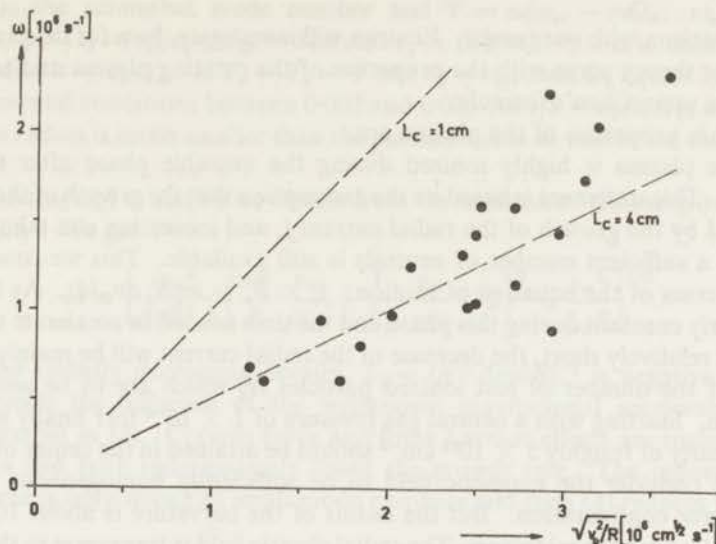


FIG. 6.—Growth rate ω vs. $\sqrt{(v_{\theta}^2/R)}$. The local gravitational acceleration v_{θ}^2/R is determined from the images. Dashed lines indicate the theoretical growth rate ω according to (2) with the characteristic length L_c equal to 1 cm and 4 cm.

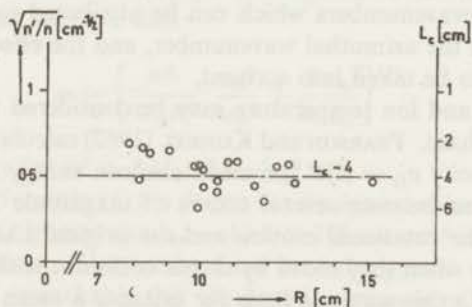


FIG. 7.—Radial dependence of the values $\sqrt{(n'/n)}$ and $L_c = n/n'$.

n'/n , is about 4 cm and independent of the radius where the plasma boundary was observed. We conclude that it is the radial dependence of the gravitational acceleration which causes the variation of the g -values within the limits mentioned above. As the measuring error in L_c can be assumed to be ± 30 per cent, it seems that the maximum gradient of the density distribution is fairly reproducible from one shot to another. The measured values up to here were only compared with the results of the common flute theory (2) where many simplifying assumptions were made. We will enlarge our discussion by including the possible influence of the Coriolis force and of finite Larmor effects at the conditions of our experiment.

5. DISCUSSION

The gravitational instability due to the rotation of a cylindrical plasma was treated by ROSENBLUTH *et al.* (1962), taking into account finite Larmor effects. The influence of the Coriolis force was in addition pointed out by CHEN (1965). This theory covers many aspects of the rotating plasma cylinder and seems to be suitable

for a comparison with our results. First we will investigate, how far the presumptions made in the theory agree with the properties of the rotating plasma and secondly we will enlarge upon Chen's formula.

The main properties of the plasma are:

(a) The plasma is highly ionized during the unstable phase after the current maximum. This statement is based on the assumption that the growth of the ionization is indicated by the growth of the radial current j_r and ionization can take place only as long as a sufficient number of neutrals is still available. This we conclude from the main terms of the equation of motion: $j_r \times B_z = m_i N_i dv_{\ominus}/dt$. As the electric field is nearly constant during this phase and the time needed to accelerate the charged particles is relatively short, the decrease of the radial current will be mainly due to the decrease of the number of just ionized particles N_i which are to be accelerated in \ominus -direction. Starting with a neutral gas pressure of 1×10^{-2} torr finally a maximum plasma density of roughly $5 \times 10^{14} \text{ cm}^{-3}$ should be attained in the center of the vessel.

(b) We consider the magnetic field to be sufficiently homogeneous though we have a mirror configuration. But the radius of the curvature is about 100 cm large at $R = 10$ cm near the midplane. The radial electric field is transverse to the magnetic field and depends on R according to Fig. 5.

(c) The plasma cylinder has a diameter of about 25 cm and an axial extension of at least the same. No disturbances in axial direction could be observed. Therefore the axial and radial wavenumbers which can be attributed to the perturbation are small compared with the azimuthal wavenumber, and the effects of axial and radial variations have not to be taken into account.

(d) The electron and ion temperature may be considered to be equal ($T_e = T_i$) during the unstable phase. PEARSON and KUNKEL (1962) calculated for a plasma which rotates with the velocity $v_D = E/B$ the mean electron energy of a near Maxwellian distribution which can become several orders of magnitude higher than the small energy only due to the rotational motion and the original Larmor movement. The electrons gain energy when they move by elastic collisions with neutrals in the direction of the E -field. In this way one finds for instance a mean energy of 2.8 eV at a drift velocity $v_D = 6 \times 10^6 \text{ cm sec}^{-1}$ ($m_e v_D^2/2 \approx 0.01 \text{ eV}$) for similar absolute values of E , B and the gas density as we have. However, we use this value for the mean electron energy only to estimate, if T_e can be set about equal to T_i . We assume that additional energy is transferred to the electrons by collisions with high energy ions ($m_i v_D^2/2 \approx 38 \text{ eV}$) as soon as the plasma density has reached its maximum value. The energy relaxation time can be estimated from Chandrasekhar's relation as referred to in ROSE and CLARK (1961). This time is $0.2 \mu\text{sec}$ at $n = 5 \times 10^{14} \text{ cm}^{-3}$ and is very short compared with the duration of the unstable phase 3.

(e) Apparently the rotating plasma is still a low β plasma as $\beta = 8nkT/B^2$ is of the order of 10^{-2} .

These properties agree well with the basic conditions of Chen's theory. We consider now the local dispersion relation for the gravitational mode of this theory which includes both, the influence of the Coriolis force and finite Larmor radius effects:

$$\Psi^2 + \left[\frac{\delta m}{r} \left(1 + \frac{\delta r}{m^2} \right) - 2 \frac{\delta r}{m} \Omega_0 \right] \Psi - \delta r \Omega_0^2 = 0 \quad (3)$$

where m is the azimuthal mode number and $\Psi = \omega/\omega_{ci} - m\Omega_0$; $\omega_{ci} = qB/m_i$; $\delta = n^{-1} dn/dr$; $\Omega_0 = v_D/v_s r$; $v_D = E/B$ and $v_s = (kT/m_i)^{1/2}$; r is in units of the ion Larmor radius $a = v_s/\omega_{ci}$. If $T_e = T_i = T$ and $v_e = v_\theta$, then Ω_0 equals $1/r$ and is at our experimental conditions between 0.007 and 0.02. As $1/r = a/R$, it is evident that the Larmor radius is much smaller than the plasma radius as well as the characteristic length L_c .

Setting $Im(\omega/\omega_{ci}) = Im(\Psi)$ we obtain from the solution of (3) the growth rate of the instability. We get

$$\omega = \left[\frac{v_\theta^2}{4m^2 L_c^2} \left(\frac{m^2}{R} \cdot \frac{v_\theta}{\omega_{ci}} + \frac{1}{L_c} \cdot \frac{v_\theta}{\omega_{ci}} - 2 \right)^2 + \frac{v_\theta^2}{L_c R} \right]^{1/2} \quad (4)$$

at which the radially decreasing density, $L_c = (n^{-1} dn/dR)^{-1}$ is negative. The last term represents the influence of the wellknown gravitational acceleration which only was present in (2). Coriolis force and finite Larmor effects are included in the other terms and both independently lower the growth rate. The influence of the Coriolis force is only strong at small mode numbers and then (4) reduces to

$$\omega = \left[\left(\frac{1}{m^2 L_c} + \frac{1}{R} \right) \frac{v_\theta^2}{L_c} \right]^{1/2} \quad (5)$$

Stability can be deduced for $m^2 < R/|L_c|$. For high mode numbers we get mainly the finite Larmor effect and we have then:

$$\omega = \left[\frac{m^2}{4L_c R^2} \cdot \frac{v_\theta^2}{\omega_{ci}^2} + \frac{1}{R} \frac{v_\theta^2}{L_c} \right]^{1/2} \quad (6)$$

what promises stability for $m^2 > 4|L_c| R \omega_{ci}/v_\theta^2$.

In Fig. 8 curves of formula (4) are drawn for the lowest value $v_\theta = 3.3 \times 10^6$ cm sec⁻¹ (curve A) and the highest value $v_\theta = 12.6 \times 10^6$ cm sec⁻¹ (curve B) as measured during the unstable phase. The curves show how the growth rate is related to the modenummer m . It is remarkable that the broad maximum of the curves A, B and of other curves which could be drawn for intermediate values of v_θ in the region in between, agrees with our observations. Mode numbers higher than $m = 20$ were never observed, which limit was certainly not determined by the optical resolution. Mostly mode number between $m = 5$ and $m = 15$ appear. Of course the modes which grow the fastest will be more often observed and will disturb the plasma boundary at a time when the slowly growing modes should become visible. Also in this region of maximum growth the stabilizing terms of equation (4) are relatively very small, so that practically no stabilizing influence exists. Therefore it seems to be correct to compare the measurements of ω with the reduced formula (2) as was done in the previous section. On the other hand for low mode numbers the growth rate is obviously reduced by the Coriolis force. This will be the reason that values below $m = 5$ could not be observed. Though the case $m = 1$ is not covered by the theory, the growth of the $m = 1$ instability as it is connected with the eccentric motion during the buildup phase, is also possibly influenced by the Coriolis force. The observed ω -values at this phase are roughly one order of magnitude smaller than they are during the later period of the high m -number instability.

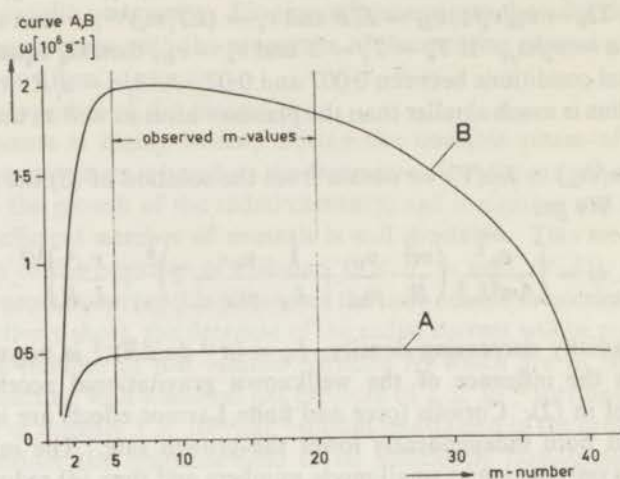


FIG. 8.—Growth rate ω as a function of the mode number m given by equation (4). The following typical values are chosen: $\omega_{st} = 4 \times 10^7 \text{ sec}^{-1}$; $R = 10 \text{ cm}$; $L_c = 4 \text{ cm}$. For the curves *A* and *B* the lower and upper limit of the observed rotational velocity v are used.

Curve *A*: $v_{\theta} = 3.3 \times 10^6 \text{ cm sec}^{-1}$.

Curve *B*: $v_{\theta} = 12.6 \times 10^6 \text{ cm}^{-1} \text{ sec}^{-1}$.

6. SUMMARY

The buildup and the unstable phase of a rotating plasma ($v_{\theta} \approx 5 \times 10^6 \text{ cm sec}^{-1}$) is discussed. In the descriptive part the operational characteristics of the discharge are explained. After a preliminary phase, when the neutral gas in front of the central electrodes becomes ionized, a central column is formed which is at the potential of the central electrodes. The further ionization takes place between this central column and the outer wall electrode after the electric field has become orthogonal to the magnetic field. Probe measurements show during the buildup phase oscillations of the local potential due to the eccentric rotation of the central plasma column. After the current maximum the radial electric field strength has nearly a $1/r$ -dependence and the oscillations have strongly decreased. Image converter pictures show the development of a high-mode instability ($m \approx 10$) at a clearly visible plasma boundary. The absence of a rigid central rod and the widely spaced electrodes are in favour of good observation.

The growth of a gravitational instability is studied in detail. The growth rate of small perturbations was measured together with the local rotational velocity. It is shown that the growth rate is proportional to the square root of the gravitational acceleration. The derived density gradient is equal to a decrease in density of one order of magnitude over a distance of 4 cm. Apart from higher mode numbers ($m > 20$) which could not be observed, the range of the preferentially observed mode numbers is in accordance with the theory by Chen on gravitational modes. The influence of the finite Larmor stabilization is small, whereas the Coriolis force for $m < 5$ can lower the growth rates and may also limit the growth of the $m = 1$ instability during the buildup phase.

Acknowledgments—The authors would like to thank Professor J. KISTEMAKER for his continuing support and valuable discussions, and Dr. F. G. INSINGER and Dr. J. G. BANNENBERG for many suggestions besides the help in engineering problems.

This work was performed as a part of the research program of the association agreement of Euratom and the "Stichting voor Fundamenteel Onderzoek der Materie" (F.O.M.) with financial support of the "Nederlandse Organisatie voor Zuiver Wetenschappelijk Onderzoek" (Z.W.O.) and Euratom.

REFERENCES

- BAKER D. A., HAMMEL J. E. and RIBE F. L. (1961) *Physics Fluids* **4**, 1534.
 BANNENBERG J. G., INSINGER F. G., RASMUSSEN C. E. and KISTEMAKER J. (1963) *Proc. 6th Int. Conf. Ioniz. Phenom. Gases, Paris*, Vol. 2, p. 393.
 BOGDANOV G. F., GOLOVIN J. N., KUCHERYAEV YU. A. and PANOV D. A. (1962) *Nucl. Fusion, Suppl.* **1**, 215.
 BOYER K., HAMMEL J. E., LONGMIRE C. L., NAGLE D., RIBE F. L. and RIESENFELD W. B. (1958) *Proc. 2nd Int. Conf. peaceful Uses atom. Energy*, Vol. 31, p. 319.
 CHEN F. F. (1965) *Physics Fluids* **9**, 965.
 GREEN T. S. and NIBLETT G. B. F. (1960) *Nucl. Fusion* **1**, 139.
 HALBACH K., BAKER W. R. and LAYMAN R. W. (1962) *Physics Fluids* **5**, 1482.
 INSINGER F. G. (1965) Thesis *Tech. Univ. Delft*.
 JOFFE M. S., SOBOLEV R. J., TEL'KOVSKIJ V. G. and YUSHMANOV E. E. (1960) *J. exp. theor. Phys.* (U.S.S.R.) **39**, 1602 and (1961) *Soviet Phys. JETP* **12**, 1117.
 LEHNERT B. (1961) *Physics Fluids* **4**, 847.
 PEARSON G. A. and KUNKEL W. B. (1963) *Phys. Rev.* **130**, 864.
 RASMUSSEN C. E., BARBIAN E. P. and KISTEMAKER J. (1969) *Plasma Phys.* **11**, 183.
 ROBERTS K. V. and TAYLOR J. B. (1962) *Phys. Rev. Lett.* **8**, 197.
 ROSE D. J. and CLARK M., JR. (1961) *Plasmas and Controlled Fusion*. Wiley, New York.
 ROSENBLUTH M. N., KRALL N. A. and ROSTOKER N., (1962) *Nucl. Fusion, Suppl.* **1**, 143.
 TOZER B. A. (1965) *Proc. IEE* **112**, 218.

CHAPTER IV

ELECTRON DENSITY MEASUREMENT USING A LASER INTERFEROMETER

1. INTRODUCTION AND THEORY

A considerable amount of time and effort was invested in our time-resolved measurement of the electron density of the plasma, by means of a laser interferometric method. We intended to perform simultaneous measurements with the laser interferometer and the image converter camera, in order to determine the density gradient in the boundary of the plasma.

It is well known, that the output of a helium-neon gas laser can be strongly influenced if the beam is reflected back into the laser cavity. The phase information, contained in the reflected beam as it enters the laser cavity may be retraced as modulations ('fringes') in the light output at the other end of the laser.

Ashby and Jephcott (1963) were first to employ this effect for the measurement of electron density in a plasma. Their experimental setup, with a plane external mirror, is shown in Fig. 1.

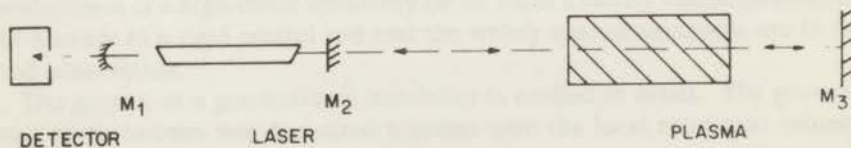


Fig. 1 - Laser interferometer for measurement of electron density in plasma.

One complete fringe is produced when the optical path length between M_2 and M_3 ,

$2 \int_{M_2}^{M_3} n dl$, where n denotes the index of refraction,

is varied by one wavelength λ_0 of the laser light in vacuo.

If the angular frequency ω of the laser light is much larger than both the plasma frequency

$$\omega_p = \left(\frac{N_e e^2}{\epsilon_0 m_e} \right)^{1/2}$$

and the electron cyclotron frequency, the index of refraction n of a highly ionized plasma is given by

$$n = \left(1 - \frac{\omega_p^2}{\omega^2} \right)^{1/2} \approx 1 - \frac{1}{2} \left(\frac{\omega_p}{\omega} \right)^2 = 1 - \frac{\lambda_0^2 e^2}{8 \pi^2 c^2 \epsilon_0 m_e} N_e \quad (1)$$

where c is the speed of light in vacuo.

If n varies by an amount Δn , the resulting variation of the optical path length is $2 \Delta n L$, L being the length of the plasma, which corresponds to a number of fringes given by

$$N = 2 |\Delta n| L / \lambda_0, \quad (2)$$

where

$$\Delta n = - \frac{\lambda_0^2 e^2}{8 \pi^2 c^2 \epsilon_0 m_e} \Delta N_e \quad (3)$$

Substitution of numerical values for the constants in Eq.

(2) gives

$$N = 8.9 \times 10^{-14} \lambda_0 L |\Delta N_e|, \quad (4)$$

if λ_0 and L are measured in cm and ΔN_e in cm^{-3} .

For a monotonous change in $N_e(t)$, the electron density at any time is directly proportional to the number of fringes observed, starting from the time t_0 where $N_e(t_0) = 0$. In this simple arrangement, however, it is impossible to distinguish the sign of the density variation, which is of particular importance in practically all experimental circumstances.

It appears from Eq. (4) that the sensitivity of the measurement (the number of fringes corresponding to a certain variation ΔN_e) increases linearly with λ_0 . Since the He - Ne laser can be made to operate simultaneously at two wavelengths (e.g. 0.6328 and 3.39 μm) by a proper choice of mirrors, it is advantageous to use the radiation at 3.39 μm for the interferences and one of the two wavelengths for the detection of the fringes.

It is difficult to estimate fractions of one fringe, because of the irregular shape of the modulated signal. The lower limit of detection corresponds to one fringe, with an accuracy of $\frac{1}{4}$ fringe. According to Eq. (4), one fringe at 3.39 μm represents an integrated density variation $|\Delta N_e| L$ of $3.3 \times 10^{16} \text{ cm}^{-2}$. Several sophisticated arrangements have been invented, combining increased sensitivity with the possibility to distinguish between increasing and decreasing plasma density (e.g. Gerardo et al. 1965, Hooper and Bekefi 1966, Baker et al. 1965, Krickler and Smith 1965). The principle underlying the last two experiments has also been employed for our measurement.

A variation of the optical path length by means of a uniform translation of the external mirror along the direction of the beam will produce a regular pattern of equidistant fringes. Any additional change of the optical path

length, e.g. by a plasma of varying density, will cause a distortion of this regular pattern : an increasing plasma density means a decreasing index of refraction (see Eq.3) which in its turn gives a larger separation of the fringes.

Let $N^0(t)$ be the number of fringes resulting from the translation alone during a time interval $(t-t_0)$, and $N(t)$ the number of fringes which is actually measured; then the change $N_e(t)$ of the electron density during this time interval is given by

$$N^0(t) - N(t) = 8.9 \times 10^{14} \lambda_0 L \Delta N_e(t). \quad (5)$$

If the starting point t_0 is chosen in such a way that $N_e(t) = 0$, it follows from Eq. (5) that $N_e(t)$ is directly proportional to the difference between N^0 and N , both measured during the time interval $(t - t_0)$. The lower limit of detection and the accuracy are greatly improved by the use of this method, since it is possible to measure shifts as small as 0.1 fringe .

If a good resolution is required, the translational speed of the moving mirror should be sufficiently high.

2. EXPERIMENTS

The system which we have chosen is somewhat similar to the arrangement of Baker et al. (1965).

In our experimental setup (schematic in Fig. 2) the regular fringe pattern was realized by means of a moving mirror system (M_4) comprising two plane mirrors mounted at right angles on a turntable, and a fixed mirror M_3 (slightly concave to compensate for the divergence of the beam).

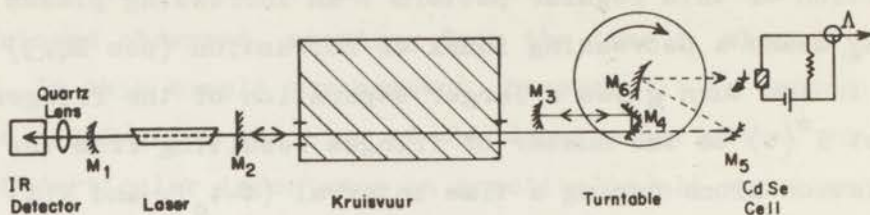


Fig. 2 - Experimental setup for time-resolved measurement of 'Kruisvuur' electron density with laser interferometer.

With this system the reflected beam could be maintained in the correct direction during 20 milliseconds; in that case a strong infrared output, exceeding the normal level by a factor 100 or even more could be observed (see Fig. 3a).

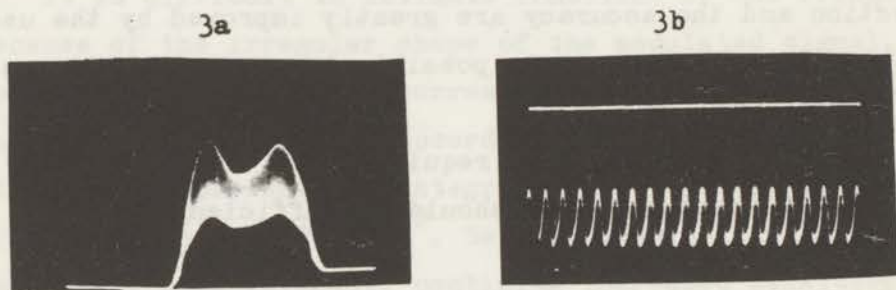


Fig. 3a - Infrared laser output without discharge.

Note the strong increment of the signal when the beam is reflected back into the laser. The fringes are not visible separately (time-scale 50msec/div.).

Fig. 3b - Same as 3a but showing regular fringe pattern (time-scale 2 μ sec/div.).

The fringes were seen as a 10 to 50 per cent modulation of this large signal. With the turntable rotating at 45 rpm a 'fringe frequency' of approx. 1 Mc/s could be attained (Fig. 3b).

The 'Bradley' Helium-Neon RF excited cw laser (maximum output 1 mW) was operated in the TEM_{00} mode with simultaneous laser action at 0.6328 and 3.39 μm , the visible beam being used for alignment and triggering purposes only. Detection of the fringes took place with a fast In-Sb infrared detector followed by a transistor amplifier. Its signal was displayed on the screen of a Tektronix type 555 dual-beam oscilloscope, together with a reference signal (usually the discharge current). Since phase modulations at $\lambda_0 = 0.6328 \mu\text{m}$ hardly affect the output at 3.39 μm , and by virtue of the insensitivity of the IR-detector to visible light, it was not necessary to use optical filters.

The laser beam passed through the discharge vessel parallel to the axis at a radius of 12 cm, since a radial passage through the midplane could not be effectuated for lack of suitable portholes.

The total path length could thus not be made smaller than 2 x 7 meters, which made the system very critical to correct alignment.

In order to minimize the influence of spurious vibrations, the whole system was mounted on two heavy concrete blocks, supported by rubber shock-absorbers. Advantage was taken of the red laser beam to trigger the electronic equipment which regulated the sequence of the discharge events.

The red light was deflected by a fixed mirror M_5 towards a mirror M_6 (see Fig. 2), positioned on the axis of the rotating turntable; the beam was thus swept along a Cd-Se photosensitive resistor, and the resulting voltage

pulse fed into the "Kruisvuur" control desk. In this way a good coincidence could be achieved between the discharge phase of interest and the time interval of 20 msec in which the regular fringe pattern was being produced.

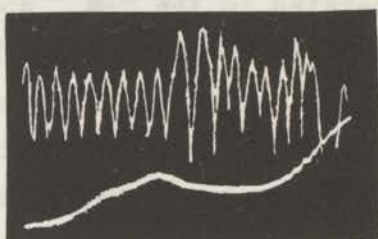


Fig. 4 - Infrared laser output during discharge.

Upper trace : laser output with fringe pattern.

Lower trace : discharge current.

Discharge conditions : $V_0 = 8$ kV, B_z ($R = 0$, $Z = 0$) = 3.8 kGauss (Time scale 2 μ s/div).

During the discharge, the expected shifts within the regular fringe pattern were indeed observed (see Fig. 4, upper trace). From this signal the fringe shift can be determined by means of a graphical method. The time at which maxima and minima occur is plotted as a function of their ordinal number. The result for the undisturbed part of the fringe pattern is a straight line, whereas a shift of the fringes shows up as a deviation from this line. The magnitude of this deviation, measured in the direction perpendicular to the time axis gives directly the fringe shift ($N^0 - N$) at any time t .

Some difficulties arose from spurious signals of small amplitude, which could be identified as electrical noise since they also appeared in the reference signal. An additional modulation of larger amplitude which was also ob-

served (see Fig. 4), did not interfere seriously with our measurements. We could not easily explain this phenomenon, since it was concluded from a separate measurement that radiation emitted by the plasma did not produce an effect of this magnitude.

Fig. 5 shows the fringe shift ($N^0 - N$), measured from Fig. 4 for the maxima and minima separately. A shift of 1.1 fringe, corresponding to an integrated electron density of $3.6 \times 10^{16} \text{ cm}^{-2}$, was reached after the first current maximum. Assuming a plasma length of half a meter, the resulting average electron density of $7.2 \times 10^{14} \text{ cm}^{-3}$ would be in reasonable agreement with the density of the hydrogen filling gas (in this case 3.3×10^{14} molecules per cm^3 in the midplane). The image converter pictures (see Chapter III, Fig. 3 and Fig. 4), which show a plasma of limited axial extension at $R = 12 \text{ cm}$, may provide some support for our estimation of the plasma length.

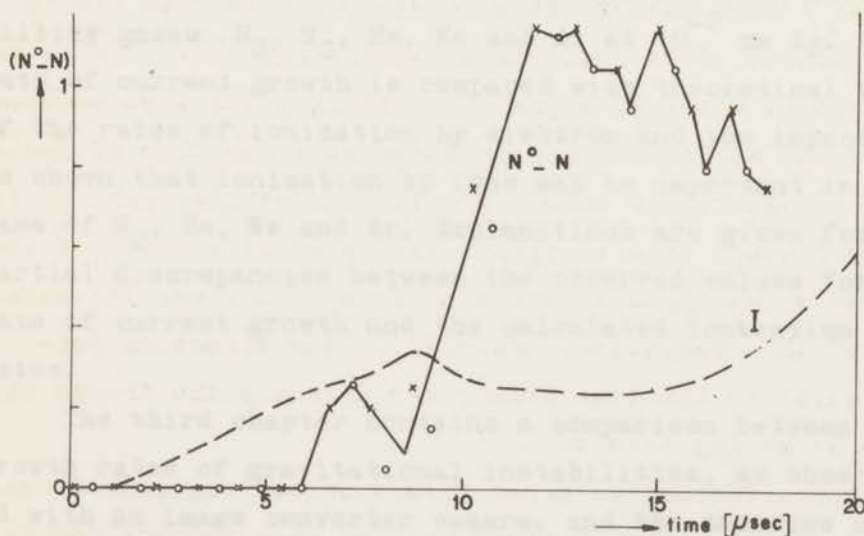


Fig. 5 - Fringe shift ($N^0 - N$) measured from Fig. 4, and discharge current I.

x — x Shift of maxima. o — o Shift of minima.

After relatively few measurements this experiment had to be discontinued because of failure of the laser tube; replacement of the tube could not be carried out in due time.

As a consequence of this, it was not possible to check our first results by comparing a large number of reliable measurements.

REFERENCES

- Ashby D.E.T.F. and Jephcott D.F. (1963) Appl. Phys. Letters 3, 13.
- Baker D.A. Hammel J.E. and Jahoda F.C. (1965) Rev. Sci. Inst. 36, 395.
- Gerardo J.B., Verdeyen J.T. and Gusinow M.A. (1965) J. Appl. Phys. 36, 3526.
- Hooper E.B. and Bekefi G. (1966) J. Appl. Phys. 37, 4083.
- Kricker W.A. and Smith W.I.B. (1965) Phys. Letters 14, 102.

SUMMARY

This thesis describes the experimental work, performed on a rotating plasma device. It may be considered as the follow-up of a thesis by F.G. Insinger (1965), from which many suggestions have been materialized.

In the first introductory chapter, a review is given of the lines which guided us to the experiments described in this thesis.

The purpose of our measurements and their place among similar experiments in other countries is briefly indicated, but is discussed in more detail in the following chapters.

Extensive information on the experimental setup is given in the chapters II and III.

The second chapter is devoted to ionization and current growth in the early stages of the discharge. An exponential increase of the current was observed with filling gases H_2 , N_2 , He, Ne and Ar at 10^{-2} mm Hg. The rate of current growth is compared with theoretical values of the rates of ionization by electron and ion impact. It is shown that ionization by ions may be important in the case of N_2 , He, Ne and Ar. Explanations are given for the partial discrepancies between the observed values for the rate of current growth and the calculated ionization rates.

The third chapter contains a comparison between the growth rates of gravitational instabilities, as observed with an image converter camera, and the theories of Lehnert and F.F. Chen.

The measured growth rate is proportional to the square root of the gravitational acceleration, whereas the range of preferentially occurring mode numbers is in accordance with Chen's theory.

Chapter IV describes a measurement of the electron density by means of a laser interferometer. It can be deduced from the few experimental data that a maximum electron density of 10^{15} cm^{-3} is reached, which corresponds to a highly or fully ionized state of the plasma.

SAMENVATTING

In dit proefschrift wordt experimenteel werk beschreven, verricht aan een roterend plasma. Het is te beschouwen als een vervolg op het werk van F.G. Insinger (1965), wiens suggesties als leidraad voor een groot deel van het hier beschreven werk hebben gediend.

In het eerste, inleidende hoofdstuk wordt een overzicht gegeven van de overwegingen en omstandigheden die tot de beschreven experimenten hebben geleid. Het doel van de metingen, en hun positie ten opzichte van soortgelijke experimenten in het buitenland worden kort omschreven. In de volgende hoofdstukken wordt hierop echter uitvoeriger ingegaan.

De hoofdstukken II en III bevatten de belangrijkste gegevens met betrekking tot de opstelling en meetapparatuur.

Hoofdstuk II is gewijd aan ionisatie en stroom aangroei in de vroege stadia van de ontlading. Met H_2 , N_2 , He, Ne en Ar als vulgas bij een druk van 10^{-2} mm kwikdruk werd een exponentiële aangroei van de ontladingsstroom waargenomen. De aangroeisnelheid werd vergeleken met de frequentie van stootionisatie door electronen en ionen. In het geval van N_2 , He, Ne en Ar blijkt ionisatie door ionen belangrijk te kunnen zijn. Voor de gedeeltelijke discrepantie tussen de waargenomen stroomaangroei en de berekende ionisatiefrequenties worden enige verklaringen gegeven.

In hoofdstuk III wordt een vergelijking gemaakt tussen de aangroeisnelheid van gravitatie-instabiliteiten van het roterend plasma, waargenomen met een snelle electronische beeldversterkercamera, en de theorie van Lehnert en F.F. Chen. De gemeten aangroeisnelheid is evenredig met

de vierkantswortel van de radiale versnelling, terwijl de waargenomen golfgetallen in overeenstemming zijn met de theorie van Chen.

In hoofdstuk IV wordt tenslotte een meting van de electronendichtheid met behulp van een laser interferometer beschreven. Uithet kleine aantal verrichte metingen kon een maximale electronendichtheid van 10^{15} cm^{-3} worden afgeleid, hetgeen correspondeert met een vrijwel volledig geioniseerd plasma.

CURRICULUM VITAE

Teneinde te voldoen aan de wens van de Faculteit der Wiskunde en Natuurwetenschappen volgt hier een kort overzicht van mijn studie.

In 1956 behaalde ik het diploma HBS-b aan het St. Aloysiuscollege te 's-Gravenhage, waarna ik aan de Rijksuniversiteit te Leiden de studie in de wis- en natuurkunde begon. Het candidaatsexamen wis- en natuurkunde met bijvak sterrekunde behaalde ik in april 1960, het doctoraalexamen experimentele natuurkunde in februari 1964.

Na het candidaatsexamen werkte ik een jaar op het Kamerlingh Onneslaboratorium in de werkgroep paramagnetische relaxatie, onder leiding van Dr J.C. Verstelle. In september 1961 kwam ik op het FOM - Instituut voor Atoom- en Molecuulfysica te Amsterdam (destijds FOM - Laboratorium voor Massascheiding geheten), waar ik in de werkgroep voor Thermonucleaire Reacties TN III onder leiding van Dr Ir F.G. Insinger mijn afstudeerwerk heb verricht. Het onderwerp van mijn doctoraalscriptie was spectroscopie van waterstofplasma's, en experimenteel onderzoek van het roterend plasma met behulp van spectrografie in het zichtbare gebied en nabije ultraviolet.

Daarna werkte ik onder supervisie van mijn promotor aan de onderzoeken die in dit proefschrift zijn beschreven. Sinds april 1968 ben ik verbonden aan het Interuniversitair Reactor Instituut te Delft, als waarnemend hoofd van de Stralingsbeschermingsdienst.

DANKWOORD

Gaarne wil ik mijn dank betuigen aan allen, die hebben bijgedragen aan het tot stand komen van dit proefschrift.

Deze dank geldt in de eerste plaats mijn promotor Prof. Dr J. Kistemaker. U hebt het onderzoek van roterende plasma's, dat reeds lang Uw speciale aandacht heeft, voortdurend gesteund en gestimuleerd met nieuwe initiatieven. Mijn verblijf op het FOM-Instituut voor Atoom- en Molecuulfysica is van grote betekenis geweest voor mijn wetenschappelijke ontwikkeling.

Dr. E.P. Barbian, aan de jaren van nauwe samenwerking bij het 'Kruisvuur I' - experiment bewaar ik de beste herinneringen. In de totstandkoming van dit proefschrift hebt U een zeer groot aandeel gehad.

Dr F. G. Insinger, U hebt met Uw voorbereidende werk het pad voor mijn onderzoekingen goeddeels geëffend. Uw scherpzinnige beschouwing van het verrichte werk, en Uw directe aanpak van allerlei problemen hebben mij in hoge mate tot voorbeeld gestrekt.

Ir J.G. Bannenberg, voor Uw hulp bij de talloze, vaak omvangrijke technische problemen ben ik U veel dank verschuldigd.

De heren H.J. Timmer en J.P. van der Fluit ben ik zeer erkentelijk voor de toegewijde technische assistentie, evenals de studenten A. Baan en J.H.A. van Wakeren voor hun hulp bij een aantal metingen.

Mijn gewezen collega's van de werkgroep TN III betuig ik mijn dank voor de vruchtbare samenwerking.

De typografische verzorging van mijn proefschrift is bij Mej. J.M. de Vletter en de heren H. Luyten en F.L. Monterie (fotografisch werk) in goede handen geweest.

De leden van de Sigarenclub ben ik zeer erkentelijk voor hun aandeel in mijn wetenschappelijke en culturele vorming.

De talrijke overige medewerkers van het FOM- Instituut, die mij op enigerlei wijze behulpzaam zijn geweest geweest betuig ik mijn dank voor de goede collegiale samenwerking.

Voor zijn medewerking bij de voltooiing van dit proefschrift ben ik Dr J. Weber van het I.R.I. te Delft veel dank verschuldigd.

